Computer Aided Diagnosis System for Melanoma Lesion Detection

By

Endalkachew Wolde Bereda

A thesis submitted in partial fulfillment of the requirements for the Degree of Master of Science in Biomedical Engineering

Center of Biomedical Engineering

Addis Ababa Institute of Technology

Addis Ababa University

Advisor: Dawit Assefa (PhD)

Co-Advisors: Mengistu Kifle (PhD)

Zerihun Abebe (MD)

Addis Ababa, Ethiopia, April 2018

Declaration

I, the undersigned, declare that this thesis is my original work. It has never been presented for a degree in any other institution and that all sources of materials used in it have been duly acknowledged.

Name: Endalkachew Wolde Bereda

Signature: _____

Date: _____

This MSc thesis has been submitted for examination with my approval as an advisor.

_____

Dawit Assefa Haile (PhD)

Addis Ababa University

School of Graduate Studies

Certificate of Examination

This is to certify that the thesis prepared by Endalkachew Wolde Bereda entitled *'Computer Aided diagnosis System for Melanoma Lesion Detection'* submitted in partial fulfillment of the requirements for the degree of Master of Science in Biomedical Engineering (Bioinstrumentation and Imaging) complies with the regulations of the University and meets the accepted standards with respect to originality and quality.

Signed by the examining committee

Examiner _____Signature _____ Date _____

Examiner _____Signature _____ Date _____

Advisor _____Signature _____ Date _____

_____

Chief of Department or Graduate program coordinator

Acknowledgements

I would like to thank The Almighty God for giving me the strength, ability and opportunity to undertake this thesis and persevere and complete it satisfactorily.

It is a great pleasure to give my sincere appreciation to my advisor Dr. Dawit Assefa Haile (PhD) for his continuous guidance and encouragements. I really admire on how you put an endless effort to make this thesis a success and I thank you for that with all my heart. I would also like to thank my co-advisors Dr. Mengistu Kifle (PhD) and Dr. Zerihun Abebe (MD) for their efforts and supportive ideas.

I am also grateful to Dr. Masreshaw Demelash (PhD) for his encouragement. In addition, a thank to Mr. Daniel Moges (MSc) for his great support. Thank you my friends and colleagues for all the care and support you have given me.

I would also want to thank my loved ones, who have supported me throughout the entire process, both by keeping me harmonious and helping me putting pieces together. I will be grateful forever for your love.

Abstract

Computer Aided Diagnosis System for Melanoma Lesion Detection

Endalkachew Wolde Bereda
Addis Ababa University, 2017

Detection of skin cancer in the earlier stage is very critical. Nowadays, skin cancer is seen as one of the most hazardous form of cancers found in humans. The most common types of skin cancers are Basal Cell Carcinoma (BCC), Squamous Cell Carcinoma (SCC) and Melanoma. Among these melanoma is the deadliest type of skin cancer. The detection of Melanoma cancer in early stage can be helpful to cure it. Computer vision plays an important role in medical image diagnosis and this has been proved by many existing systems. A computer aided skin image diagnosis system has a significant potential for screening and prognosis. It is utmost important in countries where unaided visual diagnosis system is the practice and where there is insufficient number of dermatologists. This thesis presents a computer aided diagnosis system for the detection of melanoma skin cancer using a novel mathematical scheme. The proposed method uses a holistic representation of skin color images to extract useful features for use in effective segmentation of melanoma lesions. The segmentation scheme is preceded by a processing stage composed of noise filtering color space transformation. Vertex component analysis and principal component analysis are integrated to form a hybrid approach for unmixing and feature dimension reduction. An optimized feature selection technique is also used to obtain the best achievable performance in effectively detecting the lesions. Support vector machine (SVM) along with geometrical and color feature threshold values are integrated to make effective detection of melanoma lesions. The effectiveness of the developed scheme to classify lesions into benign, suspicious and malignant melanoma is found to be promising. The proposed scheme has been tested on images taken from standard dermoscopy image databases and achieved 96.4% sensitivity, 99.4% specificity, and 97.9% overall accuracy for pixel based classification of melanomas while it achieved 98% sensitivity, 100% specificity, and 98.6% accuracy for image based classification justifying it's great promises.

Table of Contents

List of figures

List of tables

List of Abbreviations

ABCD	Asymmetry, Border irregularity, Color and Diameter
ACC	Accuracy
ANC	Abundance Non negativity Constraint
ANN	Artificial Neural Network
ASC	Abundance Sum-to-one Constraint
BCC	Basal Cell Carcinoma
CAD	Computer Aided Diagnosis
CIE	International Commission on Illumination
CMYK	Cyan, Magenta, Yellow and key (black)
DNA	Deoxyribonucleic Acid
ELM	Epiluminescence Microscopy
FCM	Fuzzy C-Means
FN	False negative
FP	False positive
FSR	Fisher Score Ranking
GLCM	Grey Level Co-occurrence Matrix
HSV	Hue, Saturation and Value
HVS	Human Visual System
IDS	International Dermoscopy Society
JPEG	Joint Photographic Expert Group
JPG	Joint Photographic Group
K-NN	K-Nearest Neighborhood

LDA	Linear Discriminant Analysis
LED	Light Emitting Diodes
MRI	Magnetic Resonance Imaging
PC	Principal Component
PCA	Principal Component Analysis
PPI	Pixel Purity Index
RGB	Red, Green and Blue
ROI	Region of Interest
SCC	Squamous Cell Carcinoma
SE	Sensitivity
SP	Specificity
SRM	Structural Risk Minimization
SVM	Support Vector Machine
TFT	Trinion Fourier Transform
TN	True Negative
TP	True Positive
UV	Ultraviolet
VCA	Vertex Component Analysis
WPT	Wavelet Packet Transform
YCbCr	Yellow Complement, blue Complement and red

Chapter One

1. Introduction

1.1 Background

The skin is the largest organ of the body, with a total area of about 20 square feet. It covers the entire body and its thickness varies considerably over all parts of the body, and between men and women and the young and the old. For example the average thickness of the skin on the forearm is 1.3 mm in male and 1.26 mm in female [1]. The skin provides a protective barrier against mechanical, thermal, and physical injuries. It protects us from microbes and the elements, prevents loss of moisture due to the presence of intercellular lipids which trap water molecules in their hydrophilic region. The skin has the ability to reduce the harmful effects of ultraviolet (UV) radiation due to the pigment melanin that absorbs UV radiation, thus protecting the cell's nuclei from DNA damage. It helps regulate body temperature through changes in blood flow in the cutaneous vascular system and evaporation of sweat from the surface. The skin also synthesizes vitamin D_3 and permits the sensations of touch, heat, and cold. Skin has three layers called epidermis, dermis and hypodermis. The epidermis is the outermost layer of skin, provides a waterproof barrier and creates our skin tone. The dermis, located beneath the epidermis, contains tough connective tissue, hair follicles, and sweat glands. The deeper subcutaneous tissue is the hypoderm which is sometimes called fat layer. It is made of fat and connective tissue. The skin's color is created by special cells called melanocytes, which are located in the epidermis and produce the pigment melanin [2, 3]. Classification of the skin based on its reaction to UV radiation is shown in Table 1.1 below.

Table 1.1 Classification of the skin based on its reaction to ultraviolet radiation [4].

Type	**Definition**	**Description**
I	Always burns but never tans	Pale skin, red hair, freckles
II	Usually burns, sometimes tans	Fair skin
III	May burn, usually tans	Darker skin
IV	Rarely burns, always tans	Mediterranean
V	Moderate constitutional pigmentation	Latin American, Middle Eastern

VI	Marked constitutional pigmentation	Black

The major causes of skin diseases can be categorized into mechanical, physical, biological and chemical categories. Friction, pressure or other forms of more forceful trauma are mechanical categories that induce changes to wide range of skin cases. Heat, cold, electricity, sunlight, ultraviolet, laser radiation and high energy sources such as x rays, radium and other radioactive substances are potentially injurious to skin and to the entire body and these are actually the causes that can be categorized under physical agents. For example milder exposure to heat supervene bacterial or fungal infection, particularly in overweight and diabetic individuals, prolonged exposure to cold water or lowered temperatures causes mild to severe injury ranging from erythema to blistering, ulceration and gangrene and the majority of skin cancers are caused by exposure to UV radiation in sunlight. Biologically, exposures to bacteria, fungi, viruses or parasites may cause primary or secondary infections of the skin. Organic and inorganic chemicals are also the major source of hazards to the skin [5].

1.2 Statement of the problem

Visual assessment of skin images is often very difficult. Not only that visual inspection could be time consuming, but also it has issues like non-repetitiveness, observer variability, and also constrained accuracy. Since unaided visual inspection of the skin is often suboptimal for diagnosis of skin diseases, many different image based skin lesion acquisition methods or modalities have been developed such as Photography, Dermoscopy, Multispectral imaging, Laser-based enhanced diagnosis, Ultrasound, Magnetic resonance imaging (MRI) and the likes. These non-invasive imaging techniques have been developed to aid the skin lesion screening process. Dermoscopy involves the use of an optical instrument paired with a powerful lighting system, allowing the examination of skin lesions in a higher magnification and it provides a more detailed view of the morphological structures and patterns. Though the detection of melanoma using dermoscopy is higher than unaided observation based detection, the visual interpretation and examination of dermoscopic images can be time consuming and its accuracy significantly depends on the experience of the dermatologists. Thus, automatic diagnosis tool is essential for physicians. In this regard, computer aided diagnostics is helpful to increase the accuracy as well as the speed. Computers are not intelligent than humans but computers may be able to extract

some information, like color variation, asymmetry and texture features, that may not be readily perceived by human eyes. Computer-aided diagnosis systems of skin images have been developed in different literatures in order to support the clinical decision of dermatologists and easily trigger the detection of the highly suspicious cases by providing an accurate segmentation of the lesions. They can also be used as an additional tool by non-experienced clinicians to perform a preliminary evaluation and to improve the patient follow-up procedure [9, 10].

Most skin images have colors when generated with different modalities. In this regard, there are many computer aided diagnostic systems that have been applied in the literature to analyze the color images for use in diagnosis, grading, and other aspects with clinical significance for melanoma. Some researchers simply used change of different color spaces while others used other algorithms to extract meaningful features from such skin images including texture, pattern, and the likes. With the use of dermoscopy and several clinical algorithms such as the ABCD rule, the 7-point checklist, and the Menzies method, the diagnosis accuracy of melanoma has been higher than the simple naked-eye examination. However, clinical diagnosis is inherently subjective and complex, thus the accuracy is highly dependent on experiences of dermatologists, which is estimated to be about 75 – 85% [11]. The manual procedure is highly subjective and rarely repetitive. Several automated detection systems have been developed in the literature by researchers to reduce subjectivity and complexity of clinical diagnosis of melanoma. Most of these systems treat the skin tissue as a uniform or homogeneous medium. Nevertheless, the skin tissue is inhomogeneous with multilayered structure, which consists of two primary layers, the dermis and epidermis, which are, as explained earlier, the bottom and top layers respectively.

The major drawback of most methods which have been suggested in the literature for analyzing the color skin images is separation of the color channels/bands into monochromes and serial analysis of the bands. Not only such a scheme is computationally intensive, but also it results in color artifacts, which basically arises as a result of scalar system analysis. Serial analysis of each color band results in loss of the intrinsic inter correlation information embedded among the color bands which are essential in useful image processing applications including texture analysis, pattern recognition and many more. In this regard, there are other vectorial schemes proposed in the literature for a more holistic representation and analysis of such color images. These methods have already shown great potential in different applications of color image

analysis [12, 13, 14]. In this thesis a novel skin image analysis scheme will be developed based on the vectorial concept for use in mass screening and diagnosis of melanoma.

Three different skin images are shown in Figure1.1 for demonstration: the first one is a malignant melanoma, the middle is tinea corporis, and the last one is a basal cell carcinoma case.

Figure 1.1: Skin images: malignant melanoma (left), tinea corporis (middle) and basal cell carcinoma (right) (Courtesy of Jason R. Swanson and Jeffrey L. Melton [15]),

1.3 Objectives

- **General objectives:**
  - ✓ To develop a computer aided melanoma lesion detection system that helps physicians as a decision support for melanoma management procedures.
- **Specific objectives:**
  - ✓ To implement holistic representation of skin color images using vectorial approaches.
  - ✓ To develop an algorithm that can extract useful, robust and non-redundant textural features.
  - ✓ To develop an algorithm that accurately classifies melanoma lesions with high sensitivity and specificity.

- ✓ To investigate the effect of different color spaces in skin image analysis.
- ✓ To evaluate and compare the performance of the proposed method with other schemes which have already been suggested in the literature.

1.4 Significance of the study

The incidence of melanoma skin cancer has been increasing through time and it became a reason for the death of many people globally. The usual clinical practice of melanoma diagnosis is a visual inspection by the dermatologist and then taking a biopsy invasively. However, this diagnostic technique lacks visualization of morphological features which are not discernible by examination with the naked eye. In addition, the high cost of examinations and the lack of specialists prevent many patients from receiving effective treatment. Because of these challenges, developing image based computer aided melanoma detection system becomes very important. This helps to examine a large number of images in short time and reduces the cost and workload of dermatologists. The final decision becomes more objective than observer driven techniques. This study comprised a robust image analysis algorithm that is potentially useful in melanoma lesion detection applications aiming to deal with existing issues related to it.

1.5 Literature review

Several automated detection systems have been developed in the literature by researchers to reduce subjectivity and complexity of clinical diagnosis of melanoma. Some of the approaches that have been followed by researchers are presented below.

Nadia S. and Souhir B. [16] presented a computer-aided diagnosis system for early melanoma detection. Their work was based on a combination of region growing segmentation method and the ABCD rule which is an analytical method to classify the diagnosis as melanoma, suspicious, and benign for the given dermoscope lesion. In another study, Michal K. et al. [17] presented a melanoma recognition system on the basis of dermoscopic images. They used color images of the skin lesions and SVM classifier to distinguish melanoma from other non-melanoma lesions. They also used different descriptors for the generation of the image diagnostic features, which are helpful for the final pattern recognition.

M. Chaithanya K. et al. [18] proposed a computer aided method for detection of melanoma using different image processing tools. These image analysis tools check the various melanoma texture, size and shape parameters like asymmetry, border, color, diameter and the like. These different features were analyzed for use in image segmentation and feature extraction. The extracted features were used to classify the given skin samples as having melanoma cancer lesion or not.

Another work by Darshana K. et al. [19] proposed a computer based melanoma detection system based on various stages of detection which involve collection of dermoscopic images, filtering for removing noises, segmentation based on Maximum Entropy Thresholding, feature extraction using Gray Level Co-occurrence Matrix (GLCM), and classification using Artificial Neural Network (ANN).

Deshpande A. S. et al. [20] proposed a methodology which they claimed to be a simple detection and diagnosis system that can be used by non-experts/clinicians/doctors. In their method, images were first pre-processed by using median filter for removing noises and then segmented by using Fuzzy C-Means (FCM) and statistical texture features were extracted using the GLCM. Finally, Support Vector Machine (SVM) was applied for detection of skin cancer and skin allergy.

Manousaki A. G. et al. [21] proposed an approach that incorporates parameters of geometry, color and texture as independent covariates for discriminating melanoma from melanocytic nevi (benign pigmented moles containing melanocytes). In the work of Ganster H. et al. [22], a melanoma recognition system that involves image processing, segmentation, feature calculation and selection, as well as k-NN classification was presented. The work by Alcón J. F. et al. [23] also presented an automatic image processing system that combines the outcome of image classification with context knowledge such as skin type, age, gender to add confidence to the classification. Garnavi R. and Aldeen M. [24] presented an approach that uses border- and wavelet-based texture features and four different classifiers in diagnosis of melanoma. There were also other approaches that used decision trees, logistic regression, ANN, SVM, and the like during classification stages.

What is typical in most of the methods briefly discussed above is that analysis of the skin color images is performed on either a selected color channel in a given color space or on each

individual color components separately. The three color channels are essentially correlated with each other and such inter-correlation information intrinsically embedded in the colors contains very useful information particularly when we have to perform tasks such as texture analysis, patter recognition and the like on the color images. This calls for a more holistic approach to be employed. In this thesis the efficacy of holistic representation of colors in effective identification and segmentation of melanomas is presented incorporating useful pre-processing, feature dimension reduction and features selection strategies. The application of selected imaging features in differentiating benign skin lesions from melanomas is thoroughly investigated.

1.6 Organization of the thesis

The rest of the thesis is organized as follows:

Chapter 2 discusses the general structure of the skin and existing clinical melanoma diagnostic methods. It presents some of the common benign as well as malignant melanocytic and non-melanocytic skin lesions. Chapter 3 discusses the basic concepts of Computer Aided Diagnosis (CAD) systems and the general detection scheme of most CAD systems like preprocessing, feature extraction, feature selection, and classification of color images. Chapter 4 presents the proposed melanoma skin lesion detection and classification scheme and the steps followed. The chapter also includes discussion on performance evaluation strategies employed in this thesis. Chapter 5 discusses the data sets that have been used in the current study and the results obtained in all stages of the proposed method. Quantitative analysis is done in this chapter to evaluate the performance of the proposed method. The last chapter, Chapter 6, is about the conclusion and future works of the study.

Chapter Two

2. Skin Biology and the Skin Lesion

2.1 Skin Biology

2.1.1 General structure of the human skin

The human skin is divided into three main layers: the epidermis, dermis and hypodermis**.** Figure 2.1 shows the anatomy of the human skin.

Epidermis

Epidermis is the outermost layer of the skin. This layer consists of many special skin cells including keratinocytes and melanocytes. Keratinocytes are cells that make a special fat which gives skin its waterproof properties. The actual skin color of humans is affected by many substances, however, the single most important substance determining human skin color is the pigment melanin, which is produced within the skin in cells called melanocytes. It determines the color of darker-skinned humans. The color of people with light skin is determined mainly by the bluish-white connective tissue under the dermis and by the hemoglobin circulating in the veins of the dermis. This layer is continuously shed and replaced every 15–30 days. The epidermis is sub-divided into 5 layers. *Stratum corneum* is the outermost layer of the epidermis and it prevents invasion from foreign things, such as bugs and bacteria. *Stratum lucidum* is part of the layer which contains several clear and flat dead cells. It is a tough layer and is found in thickened skin, including the palms of the hand and soles of the feet. *Stratum granulosum* is composed of 3 to 4 layers of cells. Here, keratin is formed, which is a colorless protein important for skin strength. *Stratum spinosum* is another layer which contains cells that change shape from columnar to polygonal. Keratin is also produced here. *Stratum basale* is the deepest layer of the epidermis, in which many cells are active and dividing. The stratum basale is separated from the dermis layer by a basement membrane, which is a layer made of collagen and proteins [25, 26].

Dermis

The dermis is the second major layer of the skin. It is a thick layer made up of strong connective tissues. It is further divided into two levels; the upper is made of loose connective tissue, called the *papillary layer*, and the lower layer is made of tissue that is more closely packed, called the *reticular layer*. The dermis is made up of a matrix of collagen, elastin and network of capillaries and nerves. The collagen gives the skin its strength, the elastin maintains its elasticity and the capillary network supplies nutrients to the different layers of the skin. The dermis also contains a number of specialized cells and structures. These includes: hair follicles, sweat glands, sebaceous glands (produce sebum which helps lubricate skin & hair) and nails. It also plays a great role in controlling our skin temperature and acts as a cushion against mechanical injury. When injured the dermis heals through the formation of granulation tissue (a tissue rich in new blood vessels and many different cells). This tissue helps pull the edges of a cut or wound back together. It takes our body from 3 days to 3 weeks to form this tissue [26].

Hypodermis

The hypodermis contains 50% of our body's fat that helps insulate the body from heat and cold, provides protective padding, and serves as an energy storage area [25, 26].

Melanocytes

Melanocytes are pigment cells that are found in the basal layer of the epidermis and produce a protein called melanin, a brown pigment that is responsible for the skin coloration and protection against the harmful effects of ultraviolet (UV) light by absorbing some potentially dangerous UV radiation. It also contains DNA repair enzymes that help reverse UV damage, but in some cases a person which lacks the genes for these enzymes suffer high rates of skin cancer. Melanocytes can transfer melanin to other skin cells like keratinocytes through dendrites when stimulated by exposure to UV radiation and these cells help to strengthen the hair, nails, and the skin itself. When the skin is exposed to the sun, melanin production increases, which produces a tan and this is the body's natural defense mechanism against sunburn. However melanocytes do not always function as they should. For example there is a hereditary skin condition where melanocytes do not produce melanin and this results in the formation of white and oval shaped patches of skin

that gradually grow larger. In general, the human body has the same amount of melanocytes but differ in the amount of melanin produced by melanocytes [27].

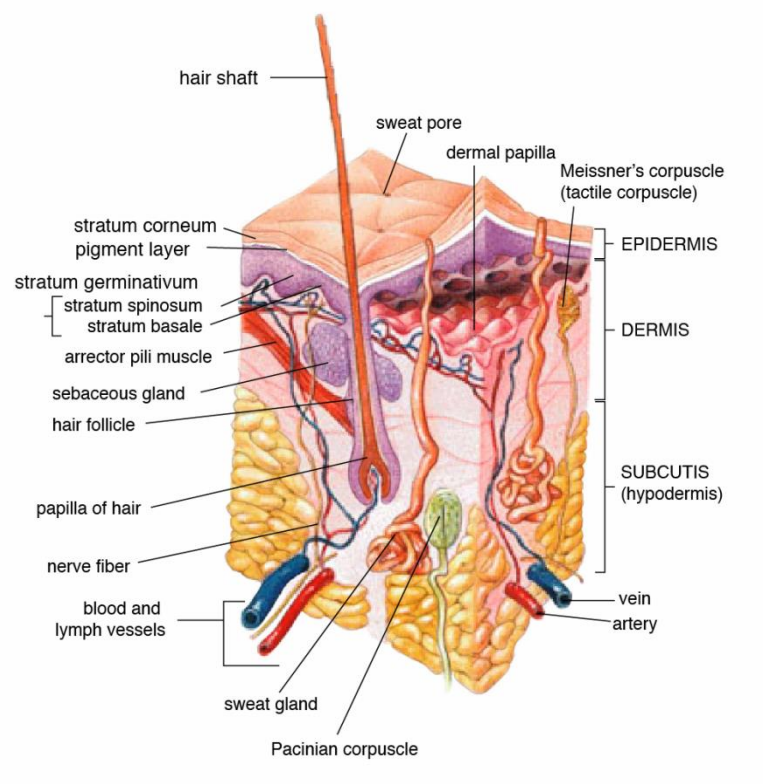

Figure 2.1: Anatomy of the skin (Courtesy of Matthew Hoffman, [3]).

2.2 The Skin Lesion

2.2.1 Benign skin lesion

Benign skin lesions can have melanocytic or non-melanocytic origins. Proliferation of melanocytes may result in congenital or acquired benign melanocytic naevi. These present as persisting macules, papules, plaques and nodules. Melanocytic lesion can be cancerous or noncancerous which are mostly described by the words malignant and benign respectively. Seborrhoeic keratosis and dermatofinroma are the most common benign non melanocytic lesions [28]. Figure 2.2 shows some examples of melanocytic and non-melanocytic benign skin lesions.

Seborrhoeic keratosis

Seborrhoeic keratosis is a benign pigmented tumor composed of epidermal keratinocytes. It resembles melanoma based on the clinical ABCD features but it is unrelated because this is benign non-melanocytic lesion.

Dermatofibroma

Dermatofibroma is a common non melanocytic benign fibrous skin lesion and it is caused by a non-cancerous growth of the dendritic cells. Benign melanocytic lesions are caused due to [31]:

- An increase in melanin within the epidermis without increasing melanocytes (ephilides);
- A temporary overproduction of melanin due to exposure to UV radiation (freckles);
- An increase in melanocytes along the basement membrane of the epidermis (lentigines); and
- Nests of melanocytes at the epidermal/dermal junction and/or within the dermis (moles).

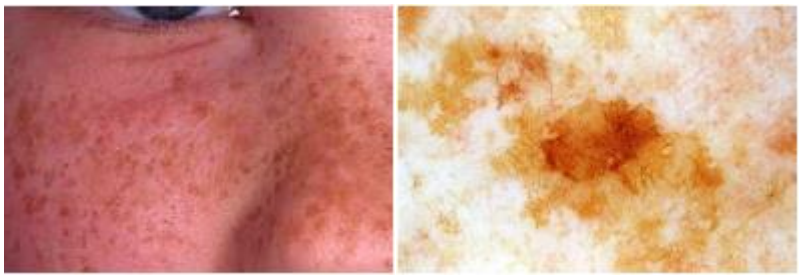

(a) Freckles (b) Lentigo (Solar)

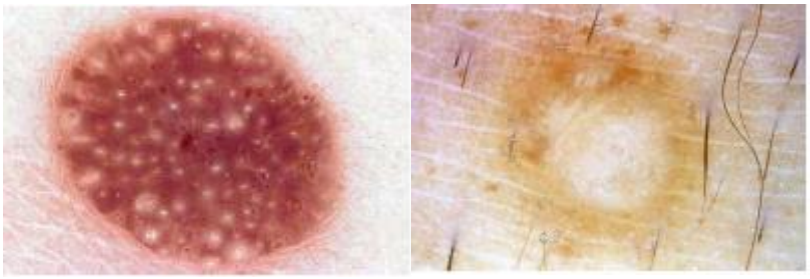

(c) Seborrhoeic Keratosis (d) Dermatofibroma

Figure 2.2 Examples of benign melanocytic and non-melanocytic lesion. (a) and (b) show examples of benign melanocytic lesions while (c) and (d) illustrate benign non-melanocytic lesions. (a) is a digital RGB image, while (b), (c) and (d) are dermoscopic images (Images courtesy of Maryam Sadeghi, [28]).

2.2.2 Skin cancer

Skin cancer is the most common type of all cancers, especially in people with light colored skin who are continuously exposed to the sun. Based on the origin, skin cancer can be categorized into melanocytic and non-melanocytic. The most common non-melanocytic skin cancers are basal cell carcinoma (BCC) and squamous cell carcinoma (SCC); melanoma is the most common malignant melanocytic skin cancer [28]. These skin cancer types are named after the skin cell in which the cancer develops. Basal cell and squamous cell carcinomas are often grouped together and called common skin cancers. Figure 2.3 shows typical examples of skin cancer lesion.

Basal cell carcinoma (BCC)

BCC begins in the basal cell layer of the skin and is the most common but least dangerous form of skin cancer. It is common in fair skinned people. It grows slowly, usually on the head, neck and upper torso where there is more exposure to sun light and may be red, pale or pearly in color. Dermatoscopic features like less white structure, blue clods, ulceration, linear serpentine vessels and indistinct border can describe BCC.

Squamous cell carcinoma (SCC)

SCC begins in squamous cells and it is very common type of cancer in people with dark colored skin, where it is mostly found in places that are not exposed to the sun such as the legs and feet. But in the case of people with fair skin it occurs in the head, face, ears, and neck. SCC is not as dangerous as melanoma but may spread to other parts of the body if not treated and it can be a thickened, red, scaly spot that may bleed easily, crust or ulcerate [5].

Melanoma

Melanoma can grow very quickly and it can become life-threatening within six weeks. Melanoma is a malignant melanocytic lesion and it can spread to other parts of the body if untreated. It causes a large majority of skin cancer deaths because of its metastasis behavior. Melanoma can appear on skin not normally exposed to the sun and it may be brown, black, blue, red or grey in color [32]; it is rare in people with dark skin and it is usually found under the fingernails and toenails, on the palms of the hands, and on the soles of the feet.

(a) BCC (b) SCC (c) Melanoma

Figure 2.3 Dermoscopy image examples of melanocytic and non-melanocytic cancer lesions: (a) and (b) are non-melanocytic cancer lesions and (c) is melanocytic cancer lesion (Images taken from Wikipedia).

Melanoma is less common but aggressive than other non-melanocytic skin cancers like BCC, SCC and rare soft tissue sarcomas. Too much exposure to solar UV-B radiation is probably the major cause for the widespread increase in the incidence of melanomas of the skin. Apart from exposure to solar radiation, no other environmental factors show a consistent association with melanoma of the skin. It arises from pigment-producing cells of the skin, usually in an existing naevus. The tumor is usually a few millimeters to several centimeters thick, that has grown in size, changed color and may bleed or ulcerate [6]. Melanoma can come up in or near to a mole, but can also appear on skin that looks quite normal. They develop when the skin pigment cells (melanocytes) become cancerous and multiply in an uncontrolled way. They can then invade the skin around them and may also spread to other areas such as the lymph nodes, liver and lungs. The risk of getting the disease is high when another family member has had melanoma and people with a damaged immune system (e.g. as a result of an HIV infection or taking immunosuppressive drugs, perhaps after an organ transplant) have also an increased chance of getting the disease. A melanoma may show one or more features like asymmetry which is actually the two halves of the area differ in their shape, the border or edges of the area may be irregular or blurred, and sometimes show notches, different shades of colors may be seen and most melanomas are at least 6 mm in diameter. Melanoma can appear on any part of the skin but they are most common in the body of men, and on the legs of women [7].

There are specific patterns/features which may represent melanomas globally or locally. The global features allow a quick preliminary categorization of a given pigmented skin lesion prior to more detailed assessment, and they are presented as arrangements of textured patterns covering

most of the lesion. The local features represent individual or grouped characteristics that appear in the lesion. Multicomponent pattern is a global feature that is most predictive for the diagnosis of melanoma, whereas the globular, cobblestone, homogeneous, and starburst patterns are most predictive for the diagnosis of benign melanocytic lesions. A typical pigmented network, irregular streaks, and regression structures are local features that show the highest association with melanoma, followed by irregular dots/globules, irregular blotches, and blue-whitish veil (See Figure 2.4). On the contrary, typical pigmented network, regular dots/globules, regular streaks, and regular blotches are mostly associated with benign melanocytic lesions [8]. Table 2.1 presents the general characteristics comparison between benign and malignant lesions.

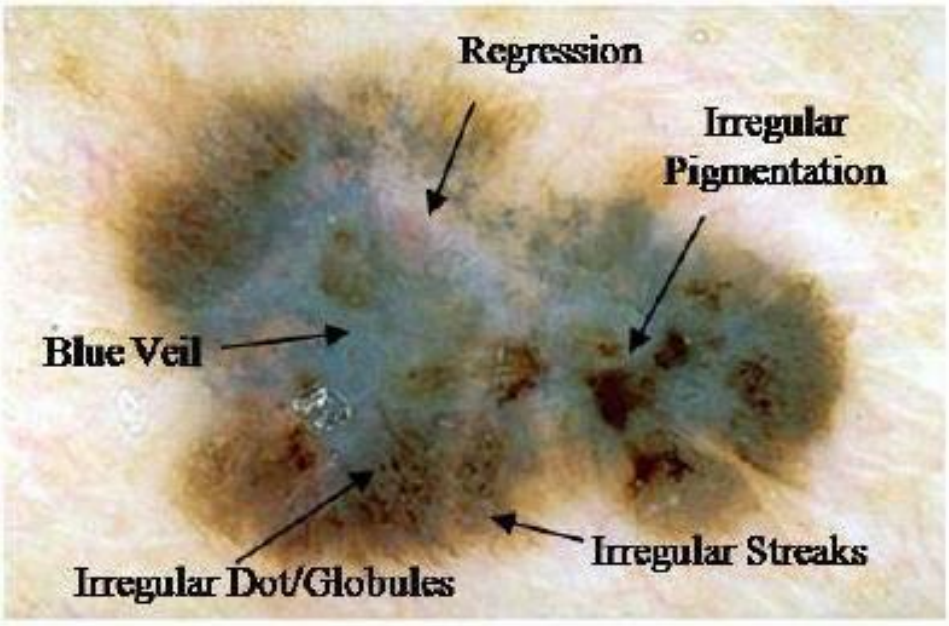

Figure 2.4: Specific features of melanoma (Image courtesy of Aurora S. et.al, [8]).

Table 2.1: Characteristics comparison between benign and malignant lesions [29].

Characteristic	Benign lesion	Malignant Lesion
Growth	Not growing	Growing-either slowly or rapidly
Bleeding	Absent	Present
Scabbing	No scab	Scab or keratin 'crust'
Number/location	Many other similar lesions	On a sun exposed area of the body
Shape	Regular shape with smooth outline or line of symmetry	Irregular outline with no symmetry
Color	Uniform pigmentation	Variation in color throughout the lesion
Occurrence	Present for many years	New lesion

2.3 Existing clinical melanoma diagnostic methods

Clinically in the past, most physicians checked the skin moles by naked eyes and clinical experience. These days a magnifying instrument called dermoscope, that uses epiluminescence microscopy (ELM) images, is used to refine the diagnosis. Biopsy is recommended if something suspicious is found while diagnosis. Dermoscope could help dermatologists to assess and extract much more information from the skin lesion. Pattern analysis was the first dermoscopic method presented for diagnosis of pigmented skin lesions [25] and it has been further modified and refined by the International Dermoscopy Society (IDS). The other methods are ABCD rule, Menzies method and the 7-point checklist (7PCL). These methods attempt to simplify the pattern analysis method by analyzing only a small subset of dermoscopic structures and create a scoring system and this lowers their accuracy from the full system pattern analysis [28].

Pattern Analysis

Diagnosis based on pattern analysis needs critical assessment of the dermoscopic structures (features) that are seen in a pigmented skin lesion, since many patterns have dermoscopic structures. The first thing to do is check if there is a pigmented structure or not.

Benign and malignant melanoma has their own characteristic features that are discriminated by the colors, architecture, symmetry and homogeneity. Table 2.2 presents the dermoscopic differentiations between benign and melanoma lesions using pattern analysis.

Table 2.2: Dermoscopic differentiations between benign and melanoma lesions using pattern analysis. Add up the score for a total of (2-17). The score of 7 or less is likely benign and the score of 8 or more is suspicious of melanoma [28].

	Low	**Medium**	**High**
Colors: few versus many light brown, dark brown, black, red, white, blue (Score 1 point for each color)	1-2 colors (1-2 points)	3-4 colors (3-4 points)	5-6 colors (5-6 points)
Architecture: order versus disorder (Score 0-2 points)	None or mild (no points)	Moderate (1 point)	Marked (2 points)
Symmetry versus asymmetry border, colors and structures (Score 0-2 points)	Symmetry in 2 axes (no points)	Symmetry in 1 axis (1 point)	No symmetry (2 points)
Homogeneity versus heterogeneity pigment network, dots/globules, blotches, regression, streaks, blue-white veil, polymorphous vessels (Score 1 point for each structure)	1 structure (1 point)	2 of structures (2 points)	3 ≥ structures (3-7 points)

ABCD rule

ABCD rule is a common feature extraction method, which helps dermatologists to recognize melanoma in its early stages. ABCD describes the clinical features of melanoma using parameters A (standing for Asymmetry), B (Border irregularity), C (Color) and D (Diameter) and these are stated as follows [28, 33]:

Asymmetry: If a lesion is symmetric (0 value) then it is benign (non-cancerous). For cancerous cases asymmetry in zero (value 1), or two orthogonal axes (value 2) are considered.

Border irregularity: The irregularity of a lesion indicates the existence of a cancer. To calculate the border, the lesion is divided into eight sections and the sharpest pattern will get the score of 1, its value ranges from 0 to 8 for the minimum and the maximum irregular borders respectively.

Colors: cancerous skin lesion's pigmentation is not uniform. The presence of up to six known colors could be detected: white, red, light brown, dark brown, slate blue, and black. Its value ranges 0 to 6, a score of 1 for the presence of each of these colors.

Diameter: The diameter that is greater than 6mm are most likely to be melanoma than the small ones.

At the end, the Total Dermoscopy Score (TDS) based on the above four parameters, is computed as follows:

$$TDS = 1.3 * A + 0.1 * B + 0.5 * C + 0.5 * D$$

If the score is less than 4.75, then the lesion is benign, if it is between 4.75 and 5.45, then it's suspicious to melanoma and if the TDS is greater than 5.45, then it is melanoma [33].

Menzies method

Menzies method classifies the dermoscopic features of benign melanocytic lesions from melanoma by two negative and positive feature sets. The negative set includes symmetry of pigmentation pattern and presence of only a single color and the positive set contains 9 positive features which are blue-white veil, multiple brown dots, pseudopods, radial streaming, scar like depigmentation, peripheral black dots/globules, multiple colors (5 or 6), multiple blue/gray dots and broad pigmentation. So for a lesion to be diagnosed as a melanoma it must have neither of both negative features and 1 or more of the 9 positive features [25].

7-point Checklist

The 7-point checklist assigns points to specific dermoscopic structures as per the checklist. It consists of 3 major features: atypical pigment network, gray-blue areas and atypical vascular pattern as well as 4 minor criteria: streaks, blotches, irregular dots and globules and regression patterns. When any of the major features is detected in a melanocytic lesion, immediate help from health professionals is recommended. When there are minor features, it is advised to be

monitored regularly. The minor criteria are worth 1 point each whereas the major are worth two. Finally a total score is computed by summing the point value based on the presence of each criterion and if the score is greater than 3, then the lesion is classified as melanoma [28].

Chapter Three

3. Computer Aided Diagnosis system

Computer aided diagnosis (CAD) system is basically a clinical decision support system, which assists doctors in the interpretation of medical images. CAD is used as a tool to provide additional information to clinicians, who will make the final decision as to the diagnosis of a patient. Its primary goal is to improve the diagnosis accuracy and consistency of clinicians by reducing the false negative rate due to observational oversight, inter-observer and intra-observer variation. Most of the time two types of general approaches are employed in CAD systems. The first one is to find the location of the lesions and the second is to quantify the image features of normal and/or abnormal patterns [34].

In general, the CAD system includes three basic components. The first is image processing which helps to enhance and extract the lesions by picking up the initial candidates of the lesions and suspicious patterns. The second is the quantification of image features such as the size, contrast, and shape of the candidates selected in the first step. Here it is important to find unique features that can distinguish reliably between a lesion and other normal anatomical structures. The third component is data processing which distinguishes between normal and abnormal patterns, based on the features obtained in the second step. The methods used in each component are discussed in the following section [34].

3.1General Detection Scheme of CAD systems

Figure 3.1 shows the general detection scheme used in CAD systems.

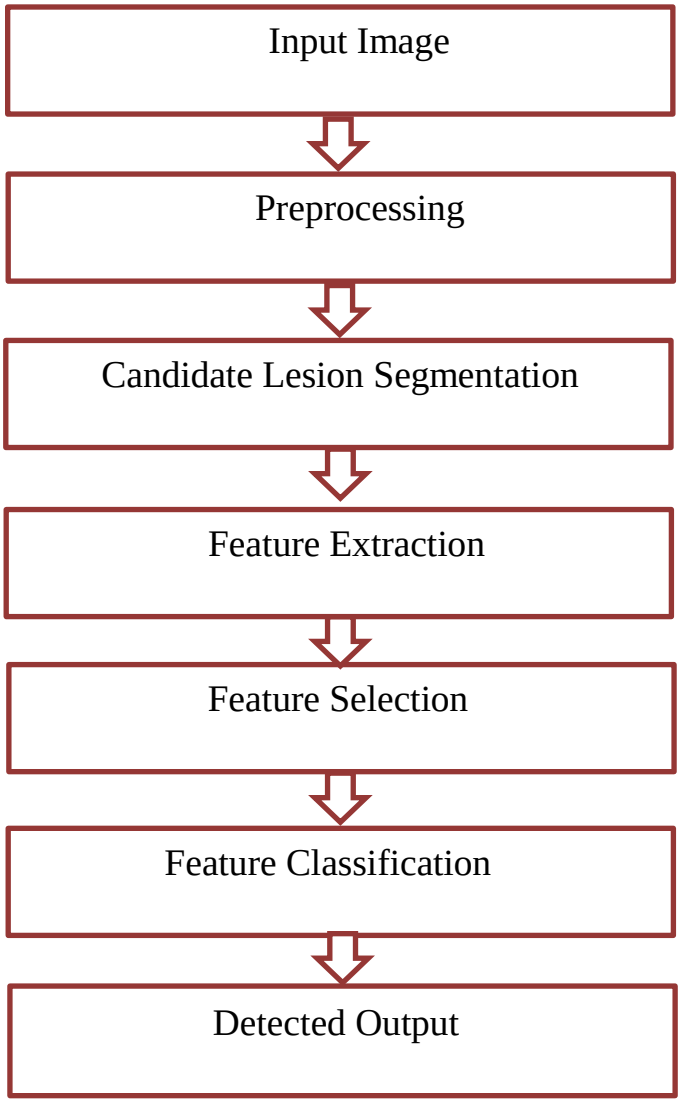

Figure 3.1: General detection scheme of CAD systems.

3.1.1Preprocessing

Image preprocessing is an essential step of detection in order to enhance the quality of original image by removing unrelated and surplus parts such as noise in the back ground of image. Thus selection of the best preprocessing techniques can greatly improve the accuracy of the CAD system. The objective of the pre-processing stage can be achieved through image enhancement and image restoration [35].

3.1.1.1 Image Enhancement

Image enhancement is an important procedure to improve the visual appearance of the image and it can be categorized into image scaling, color space transformation and contrast enhancement. The image scaling technique is applied when there is lack of same and standard size of images and this happens when the images are gathered from different sources. Color is the way the human visual system (HVS) measures a part of the electromagnetic spectrum, which ranges between 400nm and 700nm. Because of certain properties of the HVS, we are not able to see all possible combinations of the visible spectrum but we tend to group various spectra into colors [36].

A color space is a notation by which we can specify, create, and visualize colors, i.e. the human perception of the visible electromagnetic spectrum. The choice of the color space can be a very important decision which can dramatically influence the results of the processing. The knowledge of various color spaces can ease the choice of the appropriate color space. The color spaces can be classified based on perceptual linearity, intuitiveness and device dependency. Different color spaces suit for different applications. For example some equipment has limiting factors that dictate the size and type of color space that can be used. Some color spaces are perceptually linear, i.e. a 10 unit change in stimulus will produce the same change in perception wherever it is applied. Many color spaces, particularly in computer graphics, are not linear in this way. Some of them are intuitive to use, i.e. it is easy for the user to navigate within them and creating desired colors is relatively easy. Other spaces are confusing for the user with parameters with abstract relationships to the perceived color. Finally, some color spaces are tied to a specific piece of equipment (i.e. are device dependent) while others are equally valid on every device they are used [36, 38, 39].

There are many different color space like RGB, HSV, YCbCr, CMY(K), CIE XYZ, CIELab, CIELuv and others. Among those, RGB is easy to implement and it is also the most common being used in virtually every computer system, television and video. It is represented by red (R), green (G), and blue (B) chromaticity. The final color is defined by the additive combination of those three primary colors. Some authors argue that in some applications, high correlation between channels, significant perceptual non-linearity with visual perception, device dependency

and mixing of chrominance and luminance data may limit the use of the RGB space in color image processing [39].

Hue Saturation and Value (HSV) is another color space which is a non-linear transform of the RGB color space. Separation of the intensity (Value) from the chrominance information makes it advantageous in image processing. Hue describes the position of the color in a 360 spectrum. Saturation describes the pureness of the color: it measures the difference between the color and a gray scale value of equal intensity. The third channel is Value, which is the measurement of brightness. The HSV color space is also extremely intuitive. However, it is nonlinear and device dependent. It is widely used in the field of color vision. The YCbCr color space is device dependent, non-linear with human perception and unintuitive. It separates RGB to Luminance and chrominance information and useful in image compression applications. The CMY (Cyan-Magenta-Yellow) color space is a subtractive color space and is mainly used in printing applications. It is quite unintuitive and perceptually non-linear. There is also the CMYK color space where the fourth component K represents the amount of black ink.

The International Commission on Illumination (CIE) standardized the XYZ values as tristimulus values that can describe any color that can be percepted by an average human observer. A very important attribute of the CIE XYZ color space is that it is device independent. Every color space that has a transformation from the CIE XYZ color space (like CIELab, CIELuv) can also be regarded as device independent. The CIELab and CEILuv color spaces are both perceptually uniform systems, this means that the euclidian distance between two colors in the CIELuv/ CIELab color space is strongly correlated with the human visual perception [14, 39].

Contrast enhancement of images is an important step to improve the perception for further processing. It can sharpen the image border and improve the accuracy by accentuating the brightness difference between background and foreground. Linear and nonlinear contrast enhancements are the two common contrast enhancement techniques [37]. Linear contrast enhancement techniques specifically refer to contrast stretching techniques and nonlinear contrast enhancement techniques basically deal with histogram equalization.

3.1.1.2 Image Restoration

Image restoration is a process of recovering a degraded image from a blurred and noisy image. The image degradation is mainly due to imperfection of imaging system, bad focusing, and motion. Processing the corrupted image leads to fault detection, thus it is essential to know about the noise present in the image which helps to select the appropriate de-noising algorithm. The essential property of a good image de-noising method is to suppress the noise while preserving the edges. The basic de-noising methods can be classified as spatial filtering and transform domain filtering [40]. Blur is basically due to imperfect formation process of an image, which is either by bad focusing or motion between the object and camera. Most noises are filtered by this process but there are some cases, for example thick hairs in automated detection of skin cancer, which can be removed by applying other methods such as mathematical morphology methods, curvilinear structure detection and DullRazor to mention few [34].

3.1.2 Candidate Lesion Segmentation

Image segmentation is defined as the process of partitioning an image into non-overlapping, constituent regions that are homogeneous with respect to some characteristic like gray level, color, texture, brightness, contrast and other (statistical) properties. In such a way the image becomes simple and the representation can be changed into something that is more meaningful and easier to analyze. In our case, the segmentation procedure separates the lesion from the background [41]. Generally, in the case of medical imaging, the aims of segmentation include [42]:

- Studying anatomical structures;
- Identifying regions of interest, i.e. locating tumors, lesions and other abnormalities;
- Measuring tissue volume to measure growth of tumor (also decrease in size of tumor with treatment); and
- Helping in treatment planning prior to radiation therapy particularly in radiation dose calculation.

Automatic segmentation of medical images is often a difficult task as the images are complex in nature and rarely have any simple linear feature. Further, according to [42] the output of a

segmentation algorithm is affected due to partial volume effect, intensity inhomogeneity, presence of artifacts and closeness in gray level of different soft tissues.

A goal that cannot usually be achieved is to have a "perfect image segmentation", i.e. each pixel is assigned to the correct object segment. This is actually impossible because of the way a digital image is acquired, in which a pixel may straddle the "real" boundary of objects such that it partially belongs to two (or even more) objects. Most current segmentation methods do only attempt to assign a pixel to a single segment, which is an approach that is more than adequate for most applications. "Perfect image segmentation" is also often not reached because of the occurrence of over or under segmentation. Over segmentation means pixels that belong to the same object are classified as belonging to different segments. A single object may be represented by two or more segments. In the case of under segmentation, pixels that belong to different objects are classified as belonging to the same object; as a result a single segment may contain several objects [43]. As reviewed in a previous study [35] there are many medical image segmentation methods or approaches that are stated in the literature including Thresholding, Region Growing, Clustering, Classifier based, Artificial Neural Network, Deformable Model, Markov Random Field Model, Atlas-Guided, Support Vector machine, and others.

3.1.3 Feature Extraction

Object classification is usually based on the features of the pixels within the segmented regions of interest (ROIs). Therefore, the extraction of representative features of the ROIs under analysis is an important step for efficient classification process. Some of the common difficulties of this step are [44]:

- Identification of the features to be used;
- To confirm that the number of selected features are sufficient to describe the classification problem;
- The number of selected features are too large, which requires high computational resources; and
- There are redundant and/or irrelevant features that should be removed from the feature set.

However, techniques to reduce the dimensionality of the data may be used to solve these problems by just applying feature extraction and selection reduction strategies. Feature extraction is an important step in the construction of any pattern classification and aims at the extraction of the relevant information that characterizes each class. In this process relevant features are extracted from objects to form feature vectors. These feature vectors are then used by classifiers to recognize the input unit with target output unit. It becomes easier for the classifier to separate between different classes by looking at these features. Many researches were done by combining different feature vectors like shape [45], intensity [46], texture [47], and color [48] to give a better feature extraction result. Various researchers used different feature extraction approaches such as wavelet packet transform (WPT) [49, 50], grey level co-occurrence matrix (GLCM) [51, 52], Fourier power spectrum [53], Gaussian derivative kernels [54], and decision boundary feature extraction [55, 56, 57]. The GLCM approach has relatively low computational complexity and low computational time requirement [46].

3.1.4 Feature Selection

Feature selection is a process of selecting the most relevant features and reduces the dimensionality of the feature space so that irrelevant and/or redundant features are removed. However, it is important to make sure that there may not be loss of significant information in doing so. Sometimes when the number of features is small, it might be difficult to discriminate well between classes, and still a large number of features might lead to over-fitting.

There are many advantages associated with feature selection; some of them are [58]:

- Reduced feature extraction time and storage requirements;
- Reduced classifier complexity for better generalization behavior;
- Increased prediction accuracy;
- Reduced training and testing times; and
- Enhanced data understanding and visualization.

The other basic issue in feature selection is minimizing the dimensionality of pattern representation which actually results to lower computational time and less memory. The most

frequently used techniques for data classification and feature dimension reduction are Principal Component Analysis (PCA) and Linear Discriminant Analysis (LDA).

Sometimes there is also a hybrid approach, i.e. PCA + LDA. PCA is unsupervised linear method; it finds a set of the most representative projection vectors such that the projected samples preserve the most information about original samples [46]. The PCA technique basically analyzes an image's component values to obtain a new coordinate system, in such a way that the greatest variance, known as the first principal component (PC1), lies on the first axis; the second principal component (PC2) is the greatest variance in a direction orthogonal to the first axis; and the third (PC3) is orthogonal to the first and second axes. Alternatively, the principal components PC1, PC2, and PC3 can also be estimated by projecting every pixel's component values onto the three principal axes to form individual histograms for computing the corresponding variances.

LDA is a supervised linear discriminator, it uses the class information and finds a set of vectors that maximizes between-class scatter while minimizing within-class scatter. LDA attempts to express one dependent variable as a linear combination of other features or measurements. LDA is also closely related to PCA and factor analysis in that they both look for linear combination of variables which best explain the data. Their main difference is that PCA does more of feature classification whereas LDA does data classification. And also in PCA, the shape and location of the original data sets change when transformed to a different space but LDA does not change the location and it only tries to provide more class separability and draw a decision region between the given classes [59].

3.1.5 Feature Classification

Classification phase of the diagnostic system is the one in charge of making the inferences about the extracted information in the previous phases in order to be able to produce a diagnostic result of the input image. The classification process generally occurs by randomly dividing the available image samples in training and testing sets. The training step consists of developing a classification model to be used by one or more classifiers based on the samples of the training set. Each sample is composed of features extracted from a given image and its corresponding class value, which are applied as input data to the classifier for the learning process. The testing step consists of measuring the accuracy of the model learned by the training step over the test set.

In addition, such a process may present several problems concerning the dataset, such as features containing different ranges, unbalanced dataset regarding the number of samples, and/or a large number of features. Therefore, this process may require pre-processing of data, in which several methods may be applied to overcome these problems [44]. There exist different classifiers widely used in the literature such as Discriminant Analysis, Artificial Neural Network, K-Nearest Neighbourhood, Support Vector Machine, Decision Trees and others.

Chapter Four

4. Proposed Melanoma Lesion Detection Scheme

4.1 Image Acquisition

The melanoma detection scheme proposed in this thesis used images acquired using dermoscopy for testing and validation. As the name indicates dermoscopy or derm(at)oscopy is an instrument used to visualize the dermis. It is a non-invasive technique that allows a rapid and magnified in vivo observation of the skin with the visualization of morphologic features invisible to the naked eye by using skin surface microscopy [72]. Its main purpose is to evaluate lesions in order to distinguish malignant skin lesions from benign, especially in the diagnosis of melanoma. It is a hand held device which is basically composed of a high quality lens with 10 to 14-times magnification, a lighting system and rechargeable lithium battery powered [73]. This enables visualization of subsurface structures or patterns and it obviates the need for a skin biopsy for diagnosis and follow-up. The function of dermoscope is similar with a magnifying lens but it is advanced with an inbuilt illuminating system, a higher adjustable magnification, the ability to assess structures as deep as in the reticular dermis, and the ability to record images.

There exist both analog and digital dermoscopes that can give us high resolution images of skin lesions. Working in a digital platform is easier to save all the information and use it for the next steps. Figure 4.1 shows the different types of analog and digital dermoscopes that are available for use on the market. There are also advanced digital dermoscopes that can be attached to mobile phones with functionalities of sending high resolution images to specialists for expert assessment [28].

(a) (b) (c)

(d) (e)

(f) (g) (h)

Figure 4.1: Figures (a), (b), (c), (d), and (e) are analog dermoscopies and all except (a) are attachable to digital cameras to function as digital dermoscopes. Figures (f), (g), and (h) are modern digital dermoscopes (Pictures courtesy of Maryam Sadeghi, [28]).

The basic principle of dermoscopy is trans-illumination of a lesion and studying it with a high magnification to visualize subtle features. Most of the light incident on dry, scaly skin is reflected, but smooth, oily skin has improved skin translucency by applying linkage fluids and this allows most of the light to pass through it, reaching the deeper dermis. Thus it is possible to

visualize subsurface skin structures. The refracted light trans-illuminates the lesion while passing through it and is perceived as a distinct pattern (see Figure 4.2). There are various linkage fluids like oils (olive oil, mineral oil), water, an antiseptic solution, glycerin and liquid paraffin, to name a few. Water or antiseptic solutions evaporate quickly compared to other linkage fluids and hence are less preferred than oils. Liquid paraffin is actually the perfect candidate because it is inexpensive, safe and easily available, with good results. The glass plate (made of multi-coated silicone glass) used in dermoscopies has a refractive index (1.52) comparable to that of skin (1.55) and hence when placed over oil-applied skin, further enhances trans-illumination of the lesion. In the illumination system it is possible to use halogen lamps or light emitting diodes (LED), however, LED provides high intensity white light and consume 70% less power than halogen lamps. The LEDs are also designed to emit lights of different colors for better visualization of the skin since light skin penetration is proportional to the wavelength of light [73, 74].

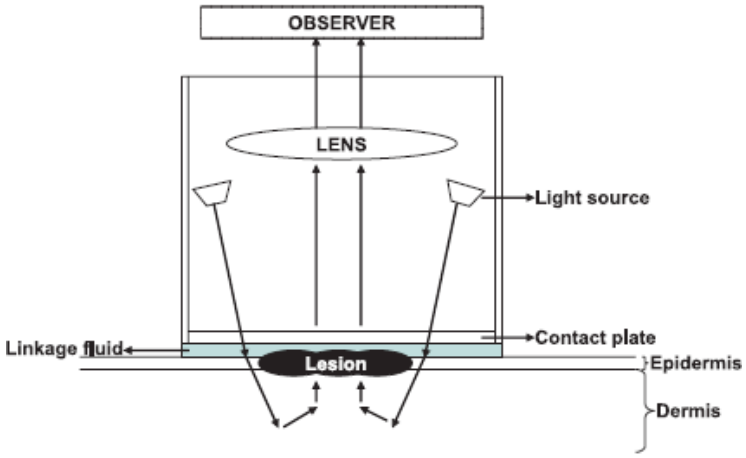

Figure 4.2: Optics of dermoscope (Courtesy of K. C. Nischal et al. [74]).

4.2 The Proposed Method

The proposed method represents and analyzes skin color images holistically in the trinion (three) space and extracts useful skin image features by applying trinion based Fourier transforms. The scheme is composed of selection of appropriate color space, dimension reduction, higher order

feature extraction and selection, and classification which are discussed in detail in the subsequent sections. Figure 4.3 illustrates an overview of the proposed image processing scheme.

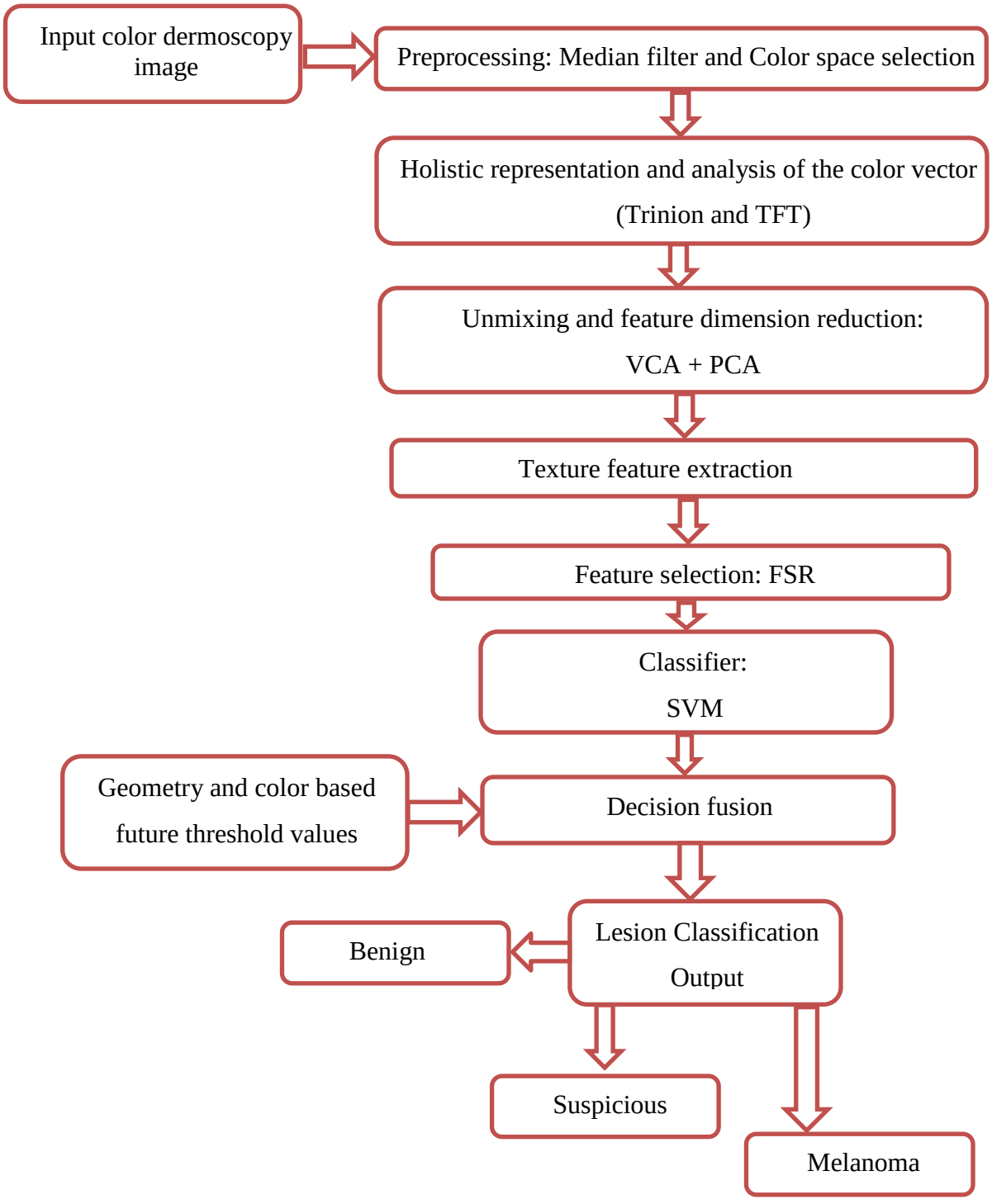

Figure 4.3: Proposed system block diagram.

4.2.1 Preprocessing

Human hair covers the entire body and has a range of different color, texture and orientation. As a result, images and lesions can become occluded by these hairs and disrupt the algorithms being used for lesion detection. Therefore hair can cause major informational corruptions when working with a skin lesion [65]. Traditionally, hair can be removed by shaving or by putting creams, but this has a problem when there is ulceration on the lesion. DullRazor is the most common method for the removal and replacement of hairs, especially the thick one, within the images [66]. In this thesis minimizing the effect of hair is addressed through the use of a 3x3 median filter on the intensity/value component of the HSV color space. Figure 4.4 presents steps of the proposed preprocessing method used in the current study.

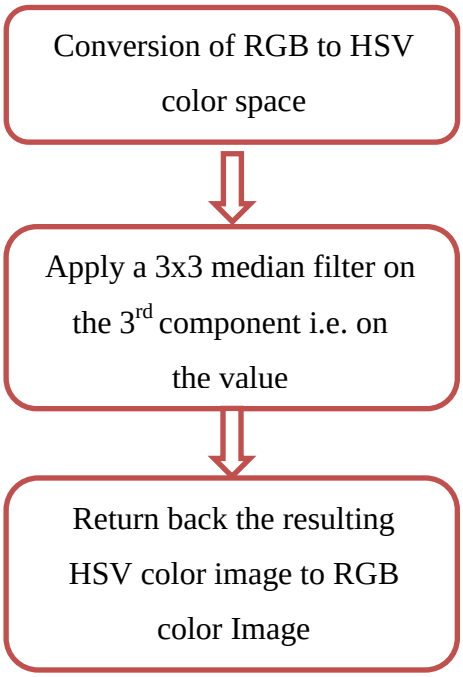

Figure 4.4: Steps of the proposed preprocessing method.

4.2.2 Vectorial color image processing in the trinion space

As reviewed in Chapter 2, there are already several methods proposed in the literature for use in analysis of skin color images. In this regard, the use of integral transforms such as the complex Fourier transform, the 2D Gabor transform, wavelets and the like have shown great promises in analyzing such images so that useful information could be traced from the images.

Traditionally, such methods are applied on the skin color images only after separation of the color components into monochromes and performing a serial analysis. The serial analysis follows similar procedures used traditionally to analyze grayscale images. Results from each color channel can then be combined afterwards and the aggregate information could be used for further image processing steps. It is not clearly known, however, how the different outputs from the different channels must be combined. There are also other schemes that use only selected color channels (in a given color space) for processing.

A major issue with the serial approach of analyzing color images is missing of the inter-correlation information embedded within the color channels. Such information is often vital in many image processing applications including texture analysis, patter recognition, spectral analysis and many more. Analyzing each color component separately could be computationally intensive at the same time. This calls for the use of a more holistic approach that does not require color band separation keeping the inter-correlation information intact. In this regard, now-a-days the use of vectorial approaches have paved a way toward effective analysis of the color images in different aspects.

One successful approach for holistic and effective representation and analysis of color images is through use of quaternions and their respective Fourier transforms. Quaternions allow vectorial representation of color pixels as a whole (as one entity) and their respective Fourier transforms allow holistic color analysis [12, 78, 79]. Quaternions are defined with one real and three imaginary components and are often considered extensions from the natural 2D complex space to a 4D space. Quaternions are used in representation of three channel color images by setting the real part equal to zero and mapping the three color channels to the three imaginary components. They have been used in applications including color auto- and cross-correlation, color edge detection, segmentation and the like.

Most color images, however, have three components, and analysis using quaternions creates redundancy and involves unnecessary extra computational cost because of the fourth component. Even though the three color channels are mapped to the three imaginary components of a quaternion, all four components will be involved during further steps of the image processing. In order to circumvent such issues with quaternions, an alternative has been suggested in the literature using trinions which are defined in three space [11]. Since their inception in 2011, trinions have been used in different applications in the color image processing world [12, 80].

A trinion is defined with one real and two imaginary components as:

$$t = a + ib + jc \tag{4.1}$$

where a, b and c are real numbers, and i, j are operators satisfying the following rules:

$$i^2 = j, ij = ji = -1, \text{and } j^2 = -i \tag{4.2}$$

The three base elements {1, i, j} of trinions form an abelian (commutative) group where 1 is the unique multiplicative identity element. Trinions are associative as well as distributive with respect to addition and multiplication; trinions are distinct from quaternions [13] for they are commutative both under addition and multiplication [13]. Any trinion number $t = a + ib + jc$ can be expressed as the sum of a real part and a vector part as:

$$t = S(t) + V(t) \tag{4.3}$$

where $S(t) = a$ is the real part of t and $V(t) = ib + jc$ is the vector part of t. It can also be written in the following form:

$$t = \left|t\right|(\cos(\phi) + \mu \sin(\phi)) \tag{4.4}$$

where $\left|t\right| = \sqrt{a^2 + b^2 + c^2}$ is the amplitude (modules), $\mu = \frac{V(t)}{|V(t)|}$ is the eigen axis, and

$\phi = arctan\frac{|V(t)|}{S(t)}$, $0 \leq \phi < \pi$ is the eigen angle (phase). When $\left|t\right| = 1$, is a unit trinion, and when $a = 0$ it becomes a pure trinion. More interesting properties of trinions could be found on the literature [13]. There are two possible working definitions of the Trinion Fourier Transform (TFT). Type I TFT is defined as:

$$T1(u,v) = \int_{-\infty}^{\infty}\int_{-\infty}^{\infty} h(x,y)(\cos(2\pi(ux+vy)) - \mu_1 \sin(2\pi(ux+vy)))\, dx\, dy \quad (4.5)$$

The inverse type I TFT (ITFT) is given by

$$h(x,y) = \int_{-\infty}^{\infty}\int_{-\infty}^{\infty} T1(u,v)(\cos(2\pi(ux+vy)) + \mu_2 \sin(2\pi(ux+vy)))\, du\, dv \quad (4.6)$$

where $h(x,y)$ is a trinion valued image function, $T1(u,v)$ is type I trinion Fourier transform of $h(x,y)$, μ_1 is a unit pure trinion and μ_2 is a trinion such that $\mu_1\mu_2 = -1$. The value of μ_1 and μ_2 are chosen arbitrarily in such a way that the resulting system $\mu_1\mu_2 = -1$ has a real valued solution.

Type II TFT is defined as follows:

$$T2(u,v) = \int_{-\infty}^{\infty}\int_{-\infty}^{\infty} h(x,y)(\cos(2\pi ux) - \mu_1 \sin(2\pi ux))(\cos(2\pi vy) - \mu_2 \sin(2\pi vy))\, dx\, dy \quad (4.7)$$

While the inverse type II TFT is given by:

$$h(x,y) = \int_{-\infty}^{\infty}\int_{-\infty}^{\infty} T2(u,v)(\cos(2\pi ux) - \mu_3 \sin(2\pi ux))(\cos(2\pi vy) - \mu_4 \sin(2\pi vy))\, du\, dv \quad (4.8)$$

where μ_1, μ_2 are unit, pure trinions and μ_3, μ_4 are trinions satisfying $\mu_1\mu_3 = -1 = \mu_2\mu_4$. Again, the choice of $\mu_1, \mu_2, \mu_3,$ and μ_4 is arbitrary. However, operations such as convolutions, autocorrelations and the likes are easier using type I TFT than type II TFT as reported previously [13], as a result type I TFT has been used in the current study after discretization. Given an NxM trinion values image function $h(x,y)$, the discrete version of type I TFT is given by:

$$T1(u,v) = \frac{1}{MN}\sum_{x=0}^{M-1}\sum_{y=0}^{N-1} h(x,y)(\cos(2\pi(\frac{ux}{M} + \frac{vy}{N})) - \mu_1 \sin(2\pi(\frac{ux}{M} + \frac{vy}{N}))) \quad (4.9)$$

A color image with three components can have different arrangements to be expressed as a trinion, i.e. any of the color channels (components) can be mapped into any of the real or vector components of a trinion.

An RGB color image is often mapped into a trinion as $h(x,y) = R + iG + jB$. It has already been shown previously that the order of the mapping of the color channels into a trinion should not affect the performance of the image analysis.

Before the mapping of the color pixels into a trinion and further processing, one has to first decide on what color space to use. The original dermoscopy images used in this thesis are in RGB format. Previous studies have used other color spaces for different applications including the Hue-Saturation-Value or HSV (and its variants: HSI, HSL, HSB), LUV, Lab and the CIE XYZ families. It is of interest in this thesis to extract texture features from the dermoscopy color skin images to accurately segment melanoma lesions. The HSV color space, for example, has been shown previously to offer good results particularly in texture analysis and synthesis [82]. For that reason, the proposed melanoma segmentation scheme has been tested in both RGB and HSV color spaces. Conversion from RGB to HSV is executed in this study using the Matlab built-in function *rgb2hsv*. A test has also been done in the LUV color space.

Similar to the RGB case, in the case of HSV too, a mapping into the trinion space is carried out by assuming the H to be the real and S and V to be the two imaginary components of a trinion. Similar mapping protocol was used in the case of LUV color space. The color image, now in the trinion space, is transformed from the spatial domain into the spatial frequency domain using the trinion Fourier transform discussed earlier. As we are looking for local textural variations within the color images, the application of the trinion Fourier transform was done locally over a translating window of size 3 by 3. Local texture features are computed accordingly preceded by other steps mentioned in the next sub sections.

4.2.3 Unmixing and feature dimension reduction

Many imaging systems have limited resolution, which causes each pixel to be a mixture of several data. So we need a mechanism to unmix the data in each pixels. Generally two models of mixing are assumed: Linear and Nonlinear mixing models.

Linear mixing model holds approximately when the mixing scale is macroscopic and there is negligible interaction among distinct endmembers. This model can be described mathematically as follows:

$$p = \boldsymbol{A} * x \tag{4.10}$$

where p represents a pixel observed by the sensor, $\boldsymbol{A}$ is a matrix of material reflectance signatures (each signature is a column of the matrix), and x is the proportion of material present in the observed pixel. This type of model is also referred to as a simplex. With x satisfying the following two constraints:

- Abundance Non negativity Constraint (ANC) - each element of x is positive.
- Abundance Sum-to-one Constraint (ASC) - the elements of x must sum to one.

Nonlinear mixing model holds when mixing scale is microscopic (or intimate mixtures), which results from multiple scattering often due to non-flat surfaces.

There are many unmixing (endmember detection) algorithms to unmix spectral data. Algorithms like Vertex Component Analysis (VCA), N-FINDR and Pixel Purity Index (PPI) assume that pure pixels (pixels which contain only one material) are present in a scene. Among these VCA has the lowest computational complexity and this actually makes VCA an effective tool to unmix spectral data [61].

Unmixing using Vertex Component Analysis

VCA is used to unmix linear mixtures of endmember spectra based on spectral dissimilarity. It is unsupervised and is based on two facts: the first is the endmembers are the vertices of a simplex and the second is the affine transformation of a simplex is also a simplex. These concepts, simplex and affine transform, are widely discussed in the literature and there is no intent in this thesis to go into depth explanation about the principles.

In VCA, each spectrum is first represented as a vector in N-dimensional space, where N is the number of color elements in each vector. If a spectrum is recorded at two frequencies, or channels, ν_1 and ν_2, then each spectrum can be represented as a two-dimensional vector in ν_1 and ν_2 space. If two spectra are identical, they will have two identical vectors; two spectra having the same composition/features but different intensities will have parallel vectors. For spectra composed of three channels/bands, in the current study for example, a quiver of vectors is obtained whose endpoints pass through a triangle; for four-dimensions the endpoints of the

vectors lie within a tetrahedron. In general, the progression from point to line, triangle and tetrahedron etc. is known in geometry as a simplex. A simplex describes a p – dimensional hull, or polytop, that possesses p+1 corners [61].

In VCA, it is assumed that the most extreme vectors in the original representation are pure component spectra, or endmembers. VCA proceeds from the original dimensionality and reduces the dimensionality step-by-step by a process known as orthogonal subspace projection. In each of these steps, the problem is reduced from a p-simplex to a (p −1)-simplex. After identifying the simplex, the VCA algorithm iteratively projects data onto a direction orthogonal to the subspace spanned by the endmembers already determined until the number of endmembers is exhausted [62].

Feature dimension reduction using Principal Component Analysis

Most of the time it's desirable to reduce the dimension of a d-dimensional dataset by projecting it onto a k dimensional subspace, where k < d, in order to increase the computational efficiency while maintaining most of the information. One way of doing that (and which has been adopted in the current study) is using Principal Component Analysis (PCA). The main goal of a PCA analysis is to identify patterns in data by detecting the correlation between variables. PCA yields the directions (principal components) that maximize the variance of the data i.e. it finds the directions of maximum variance in high-dimensional data and project it onto a smaller dimensional subspace while retaining most of the information.

Roughly speaking, given a dataset X, in PCA what we do first is obtain the Eigenvectors and Eigenvalues from the covariance matrix or correlation matrix, sort eigenvalues in descending order and choose the k eigenvectors that correspond to the k largest eigenvalues where k is the number of dimensions of the new feature subspace $k \leq d$ then we construct the projection matrix W from the selected k eigenvectors and finally transforming the original dataset X via W to obtain a k-dimensional feature subspace Y [77].

4.2.4 Feature Extraction

Texture feature analysis is frequently considered for skin image analysis. It is selected because of its assisting ability in differentiating benign from malignant lesions by measuring the roughness

of their structure. Texture descriptors with statistical, model and filter based approaches have been used for texture quantification of skin lesions [63]. It is important to extract features that are reproducible and diagnostically significant to have better diagnosis accuracy. Among the various statistical-based texture descriptors applied in the literature, the grey-level co-occurrence matrix (GLCM) proposed by Haralick et al. have been used in many literatures [64]. The GLCM calculates the co-occurrence probability matrix *p(i,j)* of each image by computing how often a pixel with certain intensity i occurs in relation with another pixel j at a certain distance d and orientation Θ.

Several measures can be computed based on the GLCM, such as variance, entropy, dissimilarity, correlation, contrast, energy, maximum probability, inverse difference, angular second moment (ASM), mean, standard deviation, homogeneity and etc. The formulae used to compute some of these statistical features are given below [20, 67, 68].

$$contrast = \sum_{n=0}^{L} n^2 \left(\sum_{i=0}^{L} \sum_{\substack{j=0 \\ |i-j|=n}}^{L} p(i,j) \right) \tag{4.11}$$

$$Variance = 0.5 * \left(\sum_{i=0}^{L} \sum_{j=0}^{L} [(i-\mu)^2 \, p(i,j) + (j-\mu)^2 \, p(i,j)] \right) \tag{4.12}$$

$$Energy = \sum_{i=0}^{L} \sum_{j=0}^{L} (p(i,j))^2 \tag{4.13}$$

$$Entropy = -\sum_{i=0}^{L} \sum_{j=0}^{L} p(i,j) * \log \mathrm{p(i,j)} \tag{4.14}$$

$$Homogeneity = \sum_{i=0}^{L} \sum_{j=0}^{L} \frac{\mathrm{p(i,j)}}{1+(i-j)^2} \tag{4.15}$$

$$Correlation = \frac{\sum_{i=0}^{L} \sum_{j=0}^{L} (i*j) * \ \mathrm{p(i,j)} - \mu_x \mu_y}{\sigma_x \sigma_y} \tag{4.16}$$

$$Cluster\ Prominence = \sum_{i=0}^{L}\sum_{j=0}^{L}(i + j - \mu_x - \mu_y)^4\, p(i,j) \tag{4.17}$$

$$Cluster\ Shade = \sum_{i=0}^{L}\sum_{j=0}^{L}(i + j - \mu_x - \mu_y)^3\, p(i,j) \tag{4.18}$$

$$Sum\ Mean = 0.5 * \left(\sum_{i=0}^{L}\sum_{j=0}^{L} i\big(p(i,j)\big) + j\big(p(i,j)\big)\right) \tag{4.19}$$

where in our case $L = 3$ and

$p(i,j)$ is the normalized spectral value

$\mu = \frac{1}{9}\sum_{i=0}^{L}\sum_{j=0}^{L} p(i,j)$ is the mean of matrix,

$\mu_x = \sum_{i=0}^{L}\sum_{j=0}^{L} ip(i,j)$ is the sum of row mean,

$\mu_y = \sum_{j=0}^{L}\sum_{i=0}^{L} jp(i,j)$ is the sum of column mean,

${\sigma_x}^2 = \sum_{i=0}^{L}(i - \mu_x)^2 \sum_{j=0}^{L} p(i,j)$ is the sum of row variance, and

${\sigma_y}^2 = \sum_{j=0}^{L}(j - \mu_y)^2 \sum_{i=0}^{L} p(i,j)$ is the sum of column variance

The values of the probability of co-occureneces, *p(i,j)*, are normally computed based on the GLCM matrix.

The GLCM approach is primarily used to analyze grayscale images. Some researchers have extended the same concept to analyze color images [81]. In this thesis work, however, a different approach was devised. The justification was that the GLCM approach mainly relies on intensity information. Colors contain more important information other than intensity only. As the intent is a more holistic approach for analyzing the colors, a different approach has been followed. Accordingly, without the need for computing the GLCM matrix, the probability values *p(i,j)* were computed locally for each trinion valued 3 x 3 images after the application of the trinion Fourier transform. After the trinion Fourier transform is computed, VCA was applied followed by PCA on each 3 x 3 output. When the resulting matrix is normalized between 0 and 1, it computes the *p(i,j)* values and these new *p(i,j)* values were the ones used to compute color textures using the same formulae used by Haralick to compute the GLCM features. When the step is repeated for each color pixel over the translating window (of size 3 x 3), we receive a texture map. Accordingly, the best feature that does its purpose in accurately detecting the melanomas based on the texture map results is considered during the next classification and segmentation steps.

4.2.5 Feature Selection

In this thesis work, best features were selected based on their efficacy in accurately classifying the dermoscopic skin color images. There are many strategies available for such feature selection [58, 69]. However due to its fast and high level of accuracy in selecting the right feature to obtain the best achievable performance in classification, Fisher score ranking technique has been used in the current study to quantify the classification accuracy. The Fisher score ranking technique calculates the difference, described in terms of mean and standard deviation, between melanoma and non-melanoma (benign) classes relative to a certain feature. The Fisher score ranking index is given by:

$$R_x = \frac{\left|\mu_{x,mel} - \mu_{x,non-mel}\right|}{\left|\sigma_{x,mel} + \sigma_{x,non-mel}\right|} \tag{4.20}$$

where, R_x is the rank of feature x, the higher the R_x the higher the difference between the values of melanoma and non-melanoma classes relative to feature x; which intern implies the two classes are highly separated. The values $\mu_{x,mel}$ and $\mu_{x,non\text{-}mel}$ are the mean values of melanoma and non-melanoma classes respectively.

$$\mu_{x,mel} = \frac{1}{N}\sum_{i=1}^{N} X_{mel}^{i} \tag{4.21}$$

$$\mu_{x,non-mel} = \frac{1}{M}\sum_{i=1}^{M} X_{non-mel}^{i} \tag{4.22}$$

X_{mel} and $X_{non\text{-}mel}$ are the training sets for melanoma and non-melanoma classes respectively while N and M are the total number of X_{mel} and $X_{non\text{-}mel}$ that are present in the training set respectively. $\sigma_{x,mel}$ and $\sigma_{x,non\text{-}mel}$ are the standard deviations of melanoma and non-melanoma classes respectively given by the following formulae:

$$\sigma_{x,mel} = \sqrt{\sum_{i=0}^{N}(i-\mu_{x,mel})^2 \sum_{j=0}^{N} p(i,j)} \tag{4.23}$$

$$\sigma_{x,non-mel} = \sqrt{\sum_{i=0}^{M}(i-\mu_{x,non-mel})^2 \sum_{j=0}^{M} p(i,j)} \tag{4.24}$$

4.2.6 Classification

In the current study the task of skin lesion detection can be formulated as a typical binary classification problem, where there are two classes for skin lesions (i.e. malignant melanoma or benign) and our aim is to assign an appropriate class label to each skin lesion of the given dermoscopic images. Among the various supervised learning classification algorithms, Support Vector Machines (SVM) classifier is used in the current study due to its outstanding generalization capability and reputation of being a highly accurate paradigm [70]. By applying a binary SVM classifier, the training samples from the two different classes are separated by a hyperplane. For a given training set, while there may exist many hyperplanes that separate the

two classes, however, the SVM classifier is based on the hyperplane that maximizes the separating margin between the two classes by mapping the input pattern into a higher dimensional space through a nonlinear mapping function. And this hyper plane can be found by a method that is based on the structural risk minimization, which minimizes the upper bound on the generalization error, this actually results to avoid over fitting.

The binary SVM classifier decision function is given by the following equation [14, 71]:

$$f(x) = sign(W^T \phi(x) + b) = \sum_{i \in s} \alpha_i y_i k(x_i, x) + b \quad (4.25)$$

where, $(W^T \phi(x) + b) = 0$ is the hyperplane that separate training samples in to two classes and it is linear in terms of the transformed data ϕ(x),

α_i are Lagrange multipliers,

x is the feature vector to be classified,

ϕ(x) is a nonlinear operator which map the input pattern x into a higher dimensional space,

i is indexes of the training sample,

s is a set of indices for which x_i is a support vector for non-zero α_i,

b is the bias,

k is the kernel function and

y_i is the label of the training sample i, i.e.

$$f(x_i) \geq 0 \; for \; y_i = +1 \quad (4.26)$$

$$f(x_i) < 0 \; for \; y_i = -1 \quad (4.27)$$

Among the various kernel functions, a linear kernel function is used due to its less classification complexities. α_i and b are automatically fit to the data by the SVM training procedure to maximize the margin.

Decision fusion

Geometrical properties of the shape and color of a lesion have a paramount diagnostic importance in the detection of melanoma. The geometrical properties considered in this study are asymmetry, border irregularity, and diameter of a lesion. The outputs of the SVM classifier along with the geometrical and color feature threshold values are integrated to make detection of melanoma in its early stage possible. Thus the output of the lesion classification can be benign, suspicious or malignant. The geometrical feature threshold value can be computed using the approach stated in section 2.3. Accordingly, when the computed index values get larger and larger the lesion resembles to be malignant.

4.3 Performance Evaluation

The two criteria mostly used for assessing the quality of a classification are discrimination and calibration. Discrimination is defined as a measure to know the well separation of two classes in the data set and calibration is defined as a measure to know the closeness probability of predicted and real model based on expert knowledge. And if a system is good in discrimination, calibration can be fixed. Some of the general measures that are commonly used to analyze the discriminatory power in different methods are Accuracy, Sensitivity, Specificity, Positive predictive value, and Negative predictive value [34]. There are terms used in defining performance evaluators like: `

- True Positive (TP): a positive label or result is detected as positive.
- False Negative (FN): a positive label is detected as negative.
- False Positive (FP): a negative label is detected as positive.
- True Negative (TN): a negative label is detected as negative.

These performance evaluators can be defined as follows [34, 60]:

- Accuracy: is the total number of correctly classified segments divided by the total number of test segments. It is defined as:

$$\text{Accuracy} = \frac{TP + TN}{TP + FP + TN + FN} \tag{4.28}$$

- Sensitivity: is referred to as the true positive rate or producer's accuracy, i.e. the proportion of actual positives, which are classified as positives. It is stated as:

$$\text{Sensitivity} = \frac{TP}{TP + FN} \tag{4.29}$$

- Specificity: is referred to as true negative rate or user's accuracy, is the proportion of actual negatives, which are classified as negatives. It is mathematically described as:

$$\text{Specificity} = \frac{TN}{TN + FP} \tag{4.30}$$

- Positive predictive value (PPV): measures the probability of actual positives which are predicted positive. It is defined as:

$$\text{PPV} = \frac{TP}{TP + FP} \tag{4.31}$$

- Negative predictive value (NPV): measures the probability of actual negatives which are predicted negative. It is stated as:

$$\text{NPV} = \frac{TN}{TN + FN} \tag{4.32}$$

Chapter 5

5. Results and Discussion

5.1 Dataset

Three data sets were obtained in order to evaluate the performance of the proposed melanoma segmentation scheme developed in this thesis. These were taken from three databases namely PH^2, DermNet NZ and Dermoscopy_Images database.

PH^2 is composed of 200 dermoscopic images, 160 are benign (which include 80 common nevi and 80 atypical nevi) and 40 melanoma lesions with their respective annotations from experts. The PH^2 database was built up through a joint research collaboration between the University of do Porto and the Dermatology service of Pedro Hispano Hospital in Portugal. The dermoscopic images were obtained under the same conditions through Tuebinger Mole Analyzer system using a magnification of 20x. The raw data images are actually given in (.bmp) file type format and they are 8-bit RGB color images with a resolution of 768 x 560 pixels. The experts used a customized software tool called DerMAT for manual segmentation and annotation of the dermoscopic images, which are gold standards used during performance evaluation of the proposed method. All the dermoscopic images are either from the skin type II or III according to the Fitzpatrick skin type classification scale [75]. Therefore, the skin colors represented in the PH^2 database may vary from white to cream white. The images of the database were carefully selected taking into account their quality, resolution and dermoscopic features. The database includes medical annotation of the images namely medical segmentation of the lesion, clinical diagnosis and dermoscopic criteria (asymmetry, colors and the presence of typical and atypical differential structures) [76]. Figure 5.1 shows typical dermoscopy image taken from the database and its medical annotation.

The second database, DermNet NZ, contains A-Z skin conditions with 135 melanoma skin lesion cases and all in RGB (.jpg) format each with dimension of 640 x 480 pixels. The third database,

the Dermoscopy Image dataset, consists of RGB images of (.jpg) format with dimension of 240 x 320 pixels each.

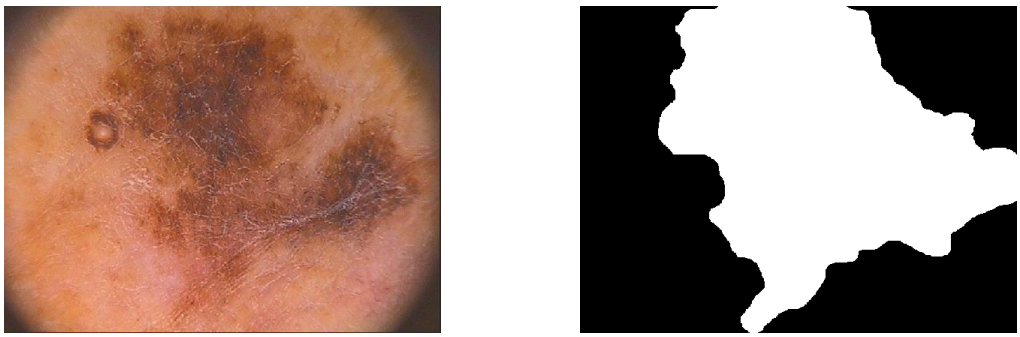

Figure 5.1: Typical dermoscopy image from the PH^2 database (left) and its medical annotation (right) (Images courtesy of Teresa et al. [76]).

5.2 Experimental results and discussion

The entire melanoma segmentation algorithm developed in this thesis has been implemented in Matlab version R2012b. The automatic classification results have been compared with the available ground truth to evaluate the performance of the proposed scheme.

5.2.1 Feature (texture) map selection for automatic melanoma detection

Best features were selected based on the generated texture feature maps (signature maps) by performing a qualitative comparison against the available gold standard provided by experts. Accordingly, four features namely: variance, contrast, sum mean and homogeneity computed in the RGB color space outperformed the rest of the features and those are the features used for final classification of the skin images. In order to quantitatively compare the classification accuracy of the different texture features computed in a given color space (in our case RGB, HSV or LUV) in terms of separating pixels of benign, suspicious or melanoma skins, F-score values were computed. Table 5.1 shows the F-score values computed with and without applying PCA for variance, contrast, sum mean and homogeneity features computed in RGB, HSV, and LUV color spaces. As shown in the table, the class separability with the application of PCA was significantly higher than without and variance feature computed over the RGB color space

resulted in the highest F-score values thus it was used for the final classification of the skin lesions. Also it could be shown from the table that features computed in the LUV color space performed much better than the same features computed in the HSV color space even though the RGB features outperformed both.

Table 5.1: Quantitative comparison of the various texture features computed in different color spaces.

Color space	Texture descriptor	F-score With PCA	F-score without PCA
RGB	Variance	21.42	2.28
RGB	Contrast	14.76	2.42
RGB	Sum mean	10.58	2.15
RGB	Homogeneity	10.87	1.84
HSV	Variance	0.75	1.71
HSV	Contrast	1.35	1.74
HSV	Sum mean	2.06	1.58
HSV	Homogeneity	3.07	1.89
LUV	Variance	9.31	20.12
LUV	Contrast	8.08	1.91
LUV	Sum mean	6.73	5.96
LUV	Homogeneity	7.07	2.40

5.2.2 Signature map results

The signature maps (feature maps) were generated by using the variance feature computed in the RGB color space. The maps were able to robustly detect melanoma regions (pixels) uniquely as dark slate gray color different from the background which appeared in cyan color. Figure 5.2 presents selected signature map outputs computed using the variance feature computed in the

RGB color space. The gold standards, which are contours from an expert, were also overlaid on the signature maps. There are regions inside the contour by the expert detected as normal (non melanoma) using the proposed method. There are also visible regions detected by the proposed algorithm to be melanomas but excluded by the expert. Such mismatches are expected when comparing manual assessments (which are subjective) to automatic approaches. But generally, we could say there is a good match between the expert contour and the melanoma signatures identified by the proposed algorithm.

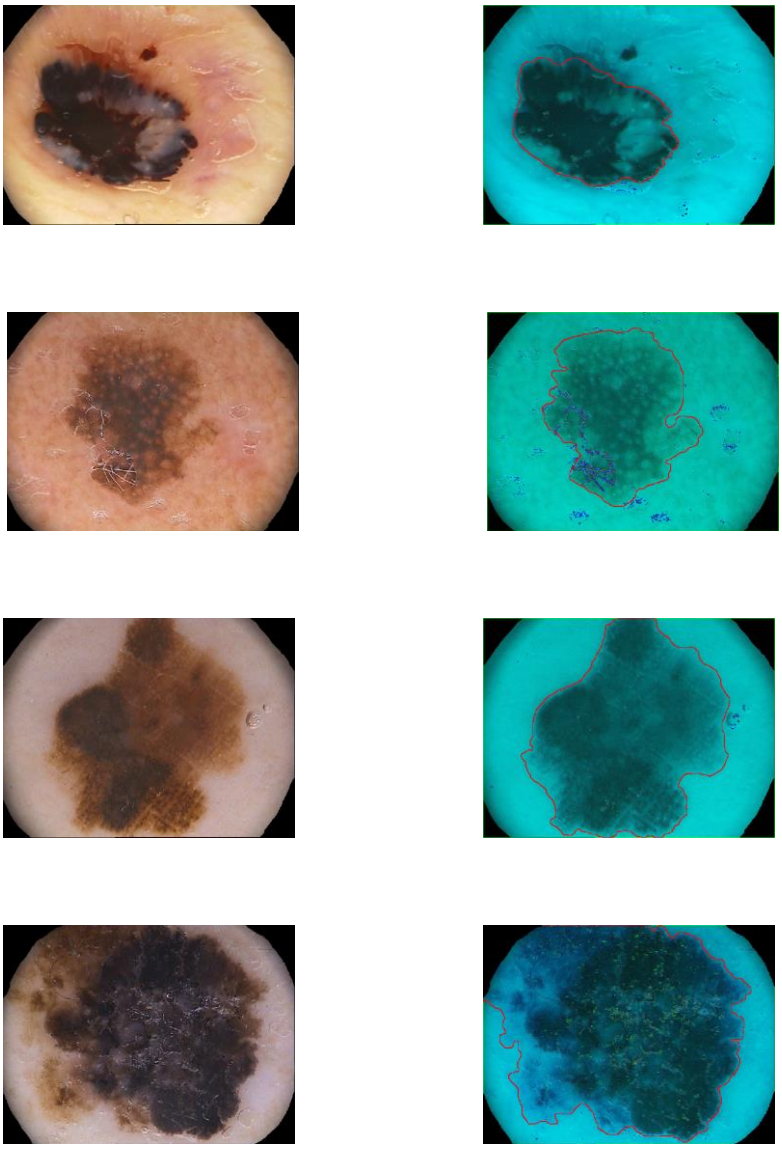

Figure 5.2: Original images (1'st column) and respective signature maps generated using the proposed scheme (2'nd column). Red lines are the ground truth annotations of melanoma.

Signature maps for benign lesions with different illumination are presented in Figure 5.3; when qualitatively analyzed, the lesions identified on the signature maps were distinct from the background skin and at the same time they were not identical in color with melanoma signature maps.

Figure 5.3: Original images (1'st column) and signature maps generated using the proposed scheme (2'nd column) for benign lesions.

5.2.3 Classification results

Figure 5.4 presents classification results applied on four typical melanoma cases. Accordingly all melanoma pixels/regions are detected as blue color on each of the respective results.

It is interesting to see such compact melanoma lesion signatures explaining the effectiveness of the proposed classification scheme. Classification results for suspicious and benign skin lesion cases are presented in Figure 5.5 and Figure 5.6 respectively. Accordingly, yellow signatures dictate suspicious pixels/regions while the benign skin cases show no distinct signatures at all and are filled with the background normal skin color signature. Note that normal skin is used as a control subject in this study.

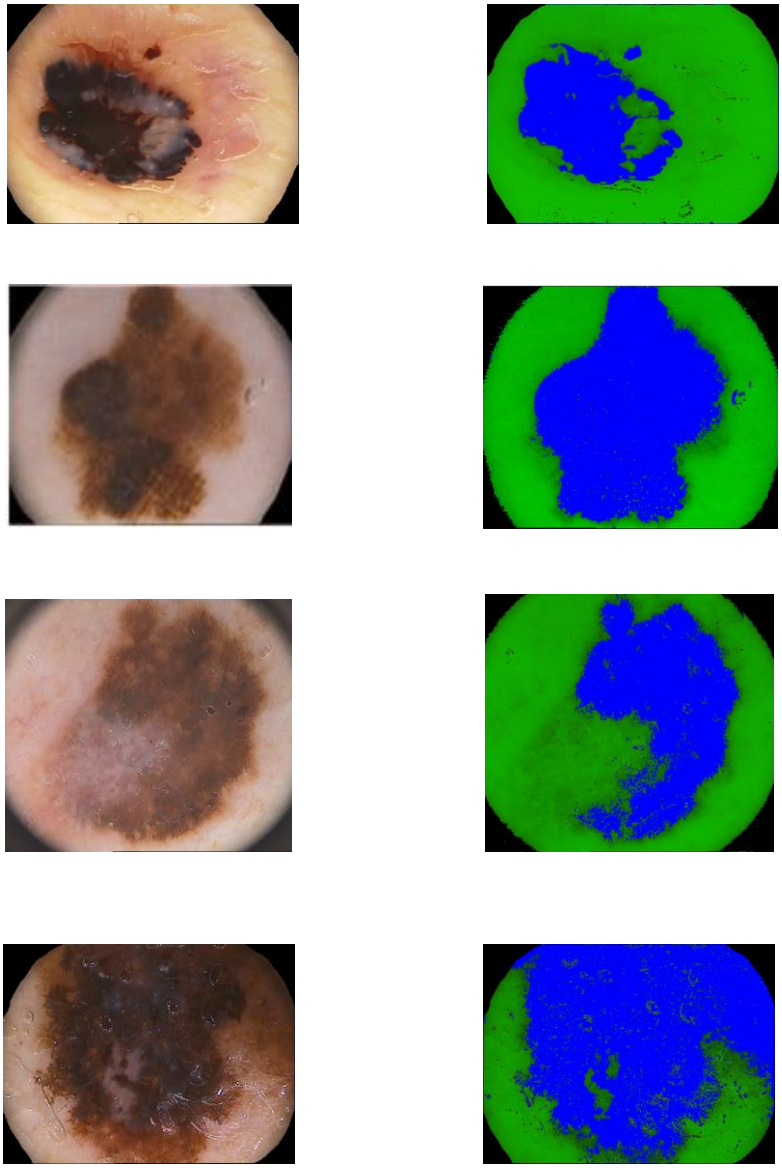

Figure 5.4: Melanoma classification results: Original lesion images (1’st column) and results after classification of melanoma pixels (2’nd column).

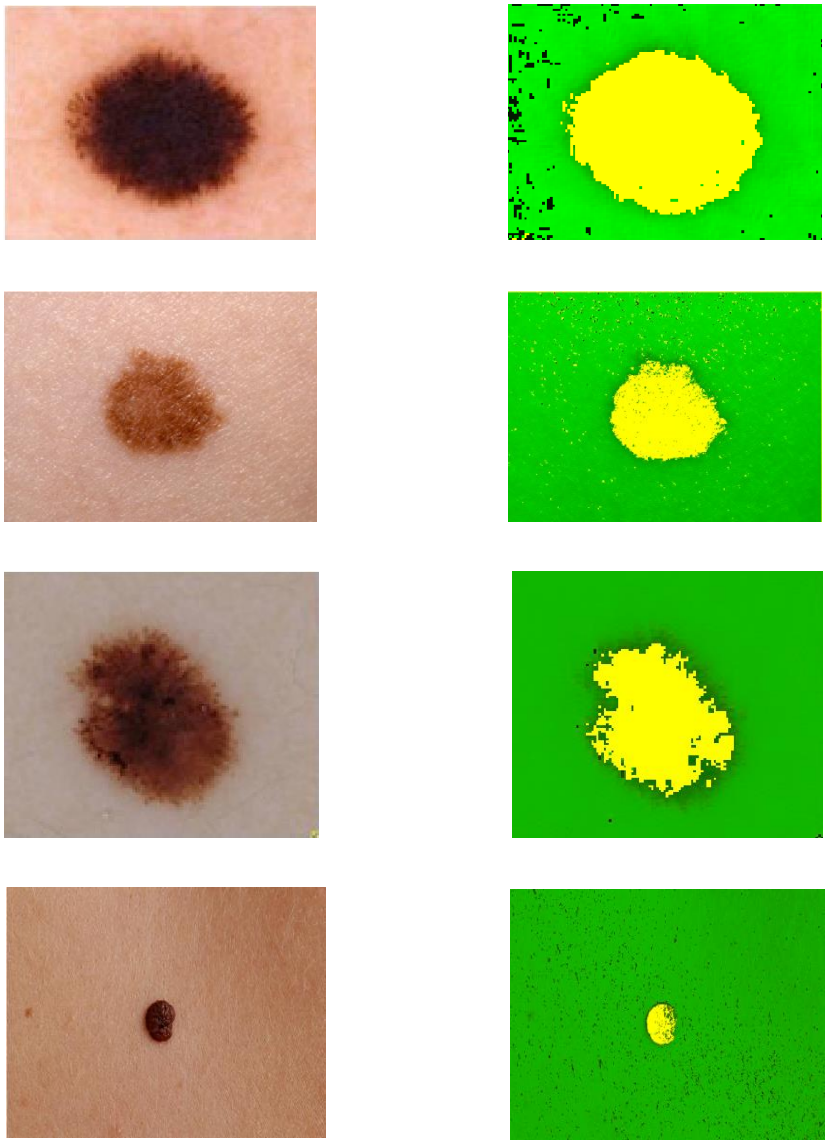

Figure 5.5: Suspicious lesion classification results: Original lesion images (1’st column) and results after classification of suspicious pixels (2’nd column).

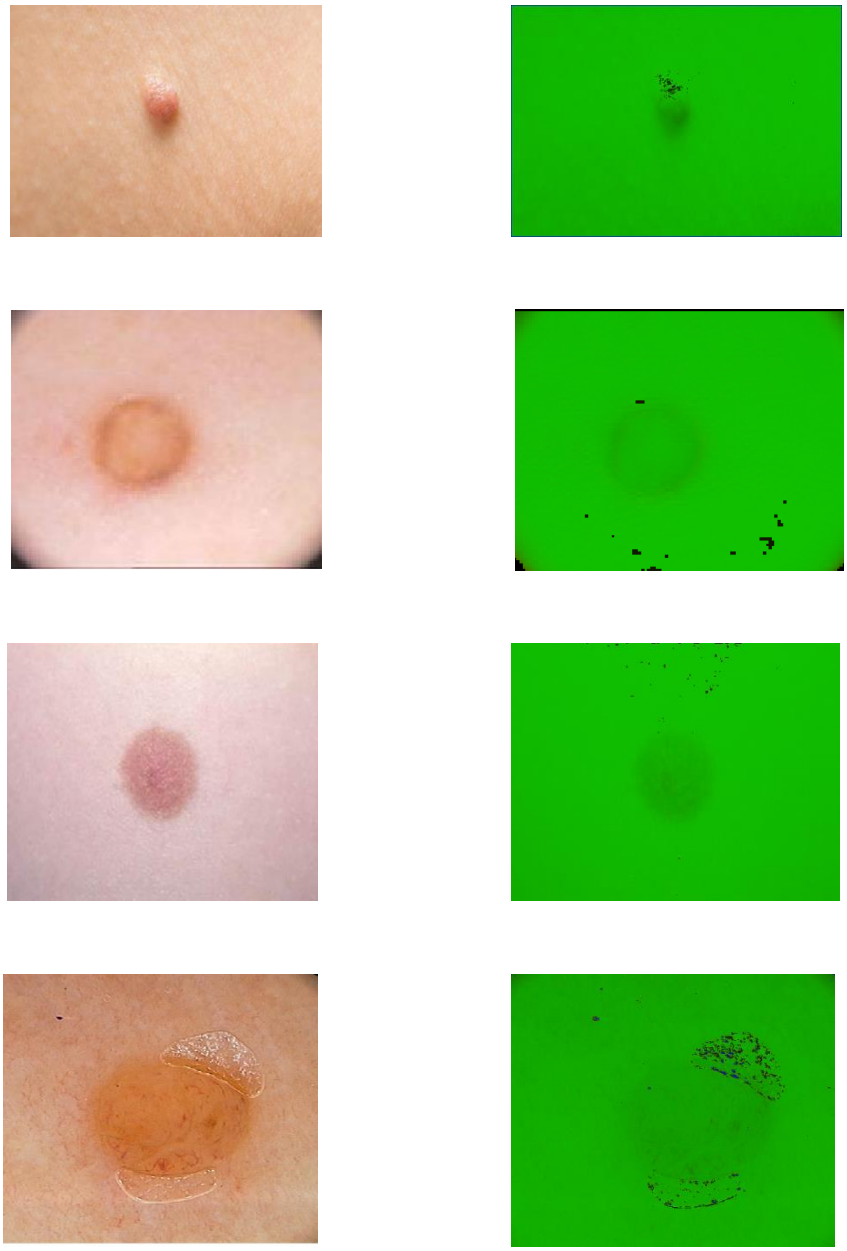

Figure 5.6: Benign lesion classification results: Original benign lesion images (1'st column) and results after classification of benign pixels (2'nd column).

Figure 5.7 presents classification results for benign lesion cases with visible hair contained in the respective skin images. As mentioned in the previous chapter, hair is considered as an artifact with a potential to affect the classification process. A median filter of size 3 x 3 was applied on the V component of the RGB skin images after conversion to HSV color space in order to smooth out the hair artifacts. Once the median filter is applied, the skin images were transformed back to the RGB space.

Even though the median filter was unable to completely avoid the hair artifacts, it is visible on the classification results that their presence did not actually affect the performance of the proposed classification scheme. Hair was uniquely detected as a dark signature after classification and with overlap neither with the benign lesion nor with the background normal skin region.

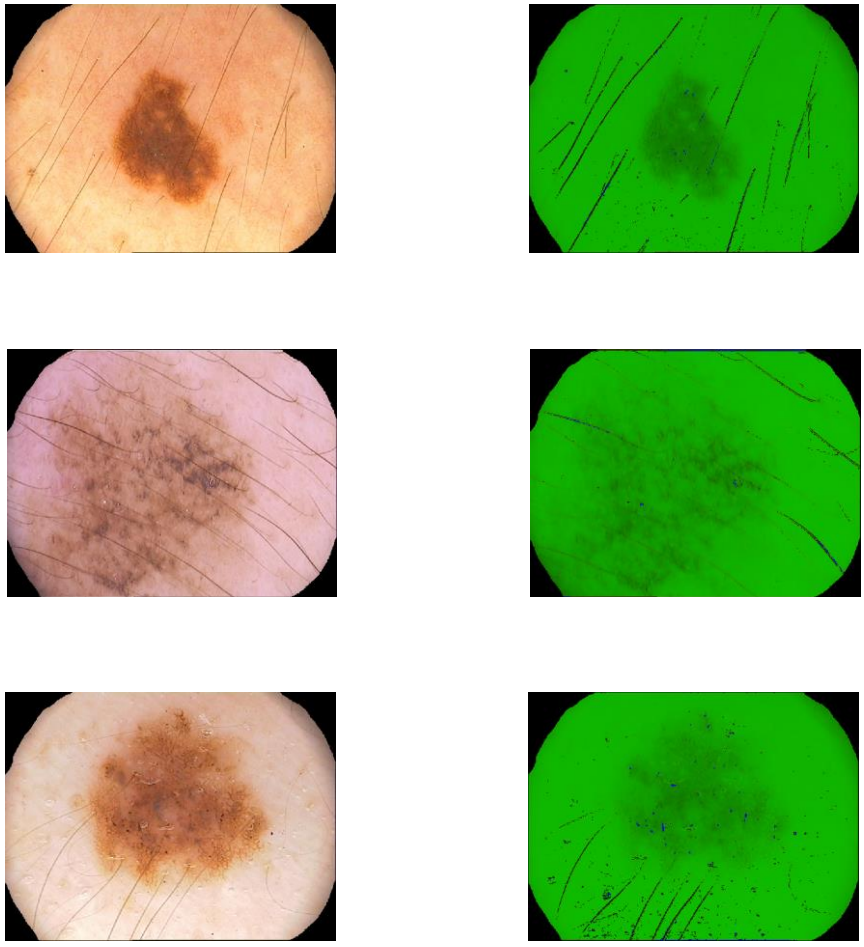

Figure 5.7: Benign lesion with hair classification results: Original benign lesion images with visible hair (1'st column) and results after classification (2'nd column).

5.2.4 System performance evaluation results

The experimental results that we have seen at different steps clearly show that the proposed method showed a great promise in automatic detection of melanoma lesions. Based on the mechanism that was stated in section 4.8, image and pixel based quantitative analysis have been done to evaluate the performance of the proposed system.

For image based classification analysis, 20 benign and 50 melanoma lesion images were taken. The proposed algorithm classified all the benign lesion images correctly, while it failed to detect only 1 melanoma lesion image resulting in an overall classification accuracy of 98.6% with 98% sensitivity, 100% specificity, 100% positive predictive value and 95.2% negative predictive value. For the pixel based criteria, a total of 83,888 pixels were taken from 10 skin lesion images. Table 5.2 summarizes different performance matrices computed for quantifying the pixel based classification accuracies of features computed using the proposed method with and without the application of PCA and VCA. In all cases SVM was used as a classifier. Accordingly, features computed using the proposed method after the application of both PCA and VCA outperformed the rest with 96.4% sensitivity, 99.4% specificity, 99.3% positive predictive value, 97% negative predictive value and 97.9% overall accuracy.

Table 5.2: Comparison of pixel based classification accuracies.

Algorithms	Acc.	SE	SP	PPV	NPV
1.Featuer with PCA & VCA	97.9%	96.4%	99.4%	99.3%	97%
2.Featuer with PCA only	89.1%	78.3%	100%	100%	98.6%
3.Feature with VCA only	83.4%	80.2%	86.6%	85.7%	84.9%

Chapter Six

6. Conclusion and recommendations

6.1 Conclusions

A great deal of work has been done in the literature to develop a CAD system to automatically detect melanoma, but most of these approaches analyze the color intensities of pigmented skin lesion images monochromatically. This thesis proposed a more holistic approach to overcome the limitations of monochromatic analysis and developed an efficient and effective melanoma lesion detection scheme. Using the proposed scheme, color skin images are represented holistically as one entity and Fourier transformed using a vectorial integral transform in three spaces making use of the trinion 'algebra'. Robust texture features were computed after the application of the trinion based Fourier transform of pre-processed color skin dermoscopic images represented in different color spaces. A hybrid approach for unmixing and feature dimension reduction (using VCA and PCA) as well as a way to extract robust higher order features were also included in the method. Several higher order texture features were computed at the end and checked for their efficacy to correctly differentiate between malignant melanomas, benign lesions as well as suspects by comparing the outputs against available ground truth information (annotations by experts). Detection of suspected lesions is meant to dictate early detection of melanomas which is badly needed in most cases. Even though different classifiers could be used, SVM was chosen for its outstanding generalization capability and reputation of being a highly accurate paradigm. Feature selection also passed through Fisher score ranking.

Based on the assessment, variance feature computed in the RGB color space was found to perform superior to the rest of the features. For both image based as well as pixel based classification criterions, the performance of the proposed method was commendable. The proposed algorithm achieved sensitivity of 96.4%, specificity of 99.4%, overall accuracy of 97.9%, positive predictive value of 99.3% and negative predictive value of 97% for pixel based classification of melanomas while for image based classification, it achieved sensitivity of 98%, specificity of 100%, overall accuracy of 98.6%, positive predictive value of 100% and negative predictive value of 95.2%. This is a commendable result when compared to other results already

reported in the literature. The results clearly demonstrated why holistic analysis of colors is more important than their serial equivalents. Conversion of colors into monochromes could be a simpler approach but comes with serious costs particularly when analyzing images generated in the medical world; the images are too sensitive and the inter-correlation information embedded within the color channels is of paramount importance, as demonstrated in the current study.

6.2 Recommendations

There might still be rooms to improve the performance of the proposed algorithm in this thesis. A better pre-processing tool to avoid artifacts such as thick hairs might be incorporated to improve the performance of the proposed scheme. The effect of illumination during image acquisition on the performance of the proposed algorithm should be rigorously checked. Important dermoscopy structures like pigment network, which are crucial for melanoma diagnosis, could be incorporated to provide the CAD system for clinical practice. Testing of the proposed melanoma detection scheme with large number of data could further confirm and validate its robustness. Translation and actual clinical evaluation of the proposed scheme might need further investigation. The proposed scheme should contribute a great deal to tele-dermatology to aid in the prevention and diagnosis of melanoma and non-melanoma skin lesions. For example, an app could be developed incorporating the proposed tool as a feature. However, such and other issues are subject to much further investigations.

References

[1] “Human skin,” Available online: https://en.wikipedia.org/wiki/Human_skin Website Referenced on January 11, 2017.

[2] Yolanda Smith, “Human Skin structure,” Available online: http://courses.washington.edu/bioen327/Labs/Lit_SkinStruct_Bensouillah_Ch01.pdf Website Referenced on November 29, 2016.

[3] Matthew Hoffman, “Picture of the skin and skin cases,” Available online: http://www.webmd.com/skin-problems-and-treatments/picture-of-the-skin#1/ Website Referenced on November 25, 2016.

[4] Jones and Bartlett "Basic Biology of the Skin," Available online: http://www.samples.jbpub.com/9780763761578/03ch_pg029-032_Wiles.indd.pdf/ Website Referenced on January 11, 2017.

[5] Donald J. Birmingham, “Occupational Skin Diseases,” Encyclopaedia of occupational Health and Safety, 2001.

[6] “Skin cancer types,” Available online: http://www.sunsmart.com.au/skin-cancer/skin-cancer-types/ Website Referenced on February 03, 2017.

[7] “Melanoma,” Available online: http://www.britishskinfoundation.org.uk/SkinInformation/AtoZofSkindisease/Melanoma.aspx/ Website Referenced on August 24, 2016.

[8] Aurora Saez, Begona Acha and Carmen Serrano, “Pattern Analysis in Dermoscopic Images,” Computer vision techniques for the diagnosis of skin cancer, series in BioEngineering, Springer, pp. 23-47, 2014.

[9] Mendonca T, Ferreira PM, Marques JS, Marcal AR, Rozeira J. “PH^2 –a dermoscopic image database for research and benchmarking,” Conf proc IEEE Eng Med Biol Soc, pp. 5437-5440, 2013.

[10] Sivangi Jain, Vandana Jagtap, Nitin Pise "Computer aided Melanoma skin cancer detection using Image processing," ICCC procedia Computer Science, pp. 735-740, 2015.

[11] Lin Li, Qizhi Zhang, Yihua Ding, Huabei Jiang, Bruce H Thiers and James Z Wand, "Automatic diagnosis of melanoma using machine learning methods on a spectroscopic system," BMC Medical Imagining, 2014.

[12] Dawit Assefa, Lalu mansinha, Kristy F. Tiampo, Henning Rasmussen, Kenzu Abdella "Local quaternion Fourier transform and color image texture analysis," Signal processing, pp. 1825-1835, 2010.

[13] Dawit Assefa, Lalu mansinha, Kristy F. Tiampo, Henning Rasmussen, Kenzu Abdella " The trinion Fourier transform of color images," Signal processing, pp. 1887-0900, 2011.

[14] Daniel Moges, Birhanu Assefa and Dawit Assefa "A mathematical Algorithm for Robust Color Retinal Image Analysis – a preliminary study," EICTAC, pp. 33-40, 2014.

[15] Jason R. Swanson and Jeffrey L. Melton "Dermatology Atlas," Available online: http://www.meddean.luc.edu/lumen/meded/medicine/dermatology/melton/title.htm
Website Referenced on December 26, 2016.

[16] Nadia Smaoui and Souhir Bessassi "A developed system for melanoma diagnosis," International Journal of Computer Vision and Signal Processing 3(1), pp. 10-17, 2013.

[17] Michal Kruk, Bartosz Swiderski, Stanislaw Osowski, jaroslaw Kurek, Monika Slowinska, Irena Walecka "Melanoma recognition using extended set of descriptors and classifiers," EURASIP Journal on Image and Video Processing, 2015.

[18] M. Chaithanya Krishna, S. Ranganayakulu, DR.P. Venkatesan "Skin Cancer Detection and Feature Extraction through Clustering Technique," IJIRCCE, Vol. 4, pp. 3736-3742, 2016.

[19] Darshana Kokitkar, Apurva Amberkar, Vaishali Giri, Prof. Krishna Tripathi "Computerized Automated Detection of Skin Cancer," IJARCCE, Vol. 5, pp. 579-581, 2016.

[20] A.S. Deshpande and Gajbar Amruta M "Automated Detection of Skin Cancer and Skin Allergy," IJARCSMS, Vol. 4, pp. 248-261, 2016.

[21] Manousaki AG, Manios AG, Tsompanaki EI, Panayiotides JG, Tsiftsis DD, Kostaki AK, Tosca AD," A simple digital image processing system to aid in melanoma diagnosis in an everyday melanocytic skin lesion unit", a preliminary report. Int J Dermatol. 2006.

[22] Ganster H, Pinz A, Rohrer R, Wildling E, Binder M, Kittler H, "Automated melanoma recognition," IEEE Trans Med Imaging. 2001.

[23] Alcón JF, Ciuhu C, Kate W, Heinrich A, Uzunbajakava N, Krekels G, Siem D, de Haan G "Automatic imaging system with decision support for inspection of pigmented skin lesions and melanoma diagnosis," IEEE J Select Top Sign Process. 2009.

[24] Garnavi R and Aldeen M, "Computer-aided diagnosis of melanoma using border- and wavelet-based texture analysis," IEEE Trans Inf Technol Biomed. 2012.

[25] "Human Skin," Virtual Medical Center, Available online: https://www.myvmc.com/anatomy/human-skin/ Website Referenced on January 12, 2017.

[26] William Montagna, F. John G. Ebling, "Human Skin," Encyclopaedia Britannica, 2017.

[27] Heather Brannon, "Understanding the Epidermis," Available online: https://www.verywell.com/anatomy-of-epidermis-1068881, Website Referenced on August 24, 2017.

[28] Maryam Sadeghi, "Towards Prevention and Early Diagnosis of Skin Cancer: Computer-Aided Analysis of Dermoscopy Images," 2012.

[29] Rodney Sinclair "Skin cancer and benign lesions," 2012.

[30] Amanda Oakley, "Principles of dermatological practice" DermNet NZ, 2008

[31] "Skin cancer types," Available online: http://www.sunsmart.com.au/skin-cancer/skin-cancer-types, Website Referenced on June 5, 2017.

[32] Farzad Nowroozipour, "Skin lesion segmentation techniques for melanoma diagnosis: comparative studies," 2016.

[33] Nilkamal S. Ramteke and Shweta V. Jain, "ABCD rule based automatic computer-aided skin cancer detection using MATLAB," Int. J. Computer technology & Applications, Vol. 4, pp. 691-697, 2013.

[34] Azadeh Noori hoshyar, "Automatic Skin Cancer Detection System," MSc dissertation, University of Technology, Sydney, 2014.

[35] Binder M, Schwarz M, Winkler A, Steiner A, Wolff K, Pehamberger H, "Epiluminescence microscopy, A useful tool for the diagnosis of pigmented skin lesions for formally trained dermatologists," Arch Dermatol. 131(3), pp. 286–291, 1995.

[36] Marko Tkalcic, prof. JurijF. Tasic, "Color Spaces," University of Ljubljana, Slovenia.

[37] J. Abdul Jaleel, Sibi Salim and Aswin R.B "Artificial Neural Network Based Detection of Skin Cancer," Int. Journal of Advanced Research in Electrical, Electronics and instrumentation Engineering, Vol. 1, pp. 200-205, 2012.

[38] Melkamu H. Asmare, Vijanth S. Asirvadam, and Lila Iznita "Color Space Selection for Color Image Enhancement Applications," IEEE: Int. Conf. on Signal Acquisition and Processing, pp. 208-212, 2009.

[39] Xi Wang, Ronny Hansch, Lizhuang Ma and Olaf Hellwich "Comparison of different color spaces for image segmentation using graph – cut," IEEE: Int. Conf. on Computer Vision Theory and Application, 2015.

[40] Mukesh C. Motwani, Mukesh C. Gadiya, Rakhi C. Motwani and Frederick C. Harris "Survey of Image Denoising Techniques," 2004.

[41] Dzung L. Pham, Chenyang Xu, and Jerry L. Prince "Current Methods in Medical Image Segmentation," Annu. Rev. biomed. Eng. pp. 315-337, 2000.

[42] Neeraj Sharma and Lalit M Aggarwal "Automated medical image segmentation techniques," Journal of Medical Physics, Vol. 35, pp. 3-14, 2010.

[43] “Segmentation,” Available online: http://www.cs.uu.nl/docs/vakken/ibv/reader/chapter10.pdf , Website Referenced on July 25, 2017.

[44] Roberta B.Oliveira, Joao P. Papa, Aledir S. Pereira and Joao Manuel R. S. Tavares “Computational Methods for Pigmented Skin Lesion Classification in Images: Review and Future Trends,” 2012.

[45] K. A. Thomas, “Image processing as applied to medical diagnostics,” MSc dissertation, University of Oregon, 2010.

[46] Sahar jafarpour, Zahra Sedghi and Mehdi Chehel Amirani “A Robust Brain MRI Classification with GLCM Features,” Int. Journal of Computer Application, Vol. 37, NO. 12, 2012.

[47] K. Wing, “Partial Differential Equation Based Methods in Medical Image Processing, PhD dissertation,” Coventry University, Philippines, 2007.

[48] T. Gevers and H. Stokman, “Classifying color edges in video into shadow-geometry, highlight, or material transitions,” IEEE Trans. Multimedia, 5(2), pp. 237-243, 2003.

[49] M. K. A. Mahmoud, A. Al-Jumaily, and M. Takruri, “The automatic identification of melanoma by wavelet and curvelet analysis: study based on neural network classification,” in Proceedings of the 11th International Conference on Hybrid Intelligent Systems (HIS ’11), pp. 680–685, 2011.

[50] G. Surowka and K. Grzesiak-Kopec,“Different learning paradigms for the classification of melanoid skin lesions using wavelets. in,” in Proceedings of the 29th Annual International Conference of the IEEE Engineering in Medicine and Biology Society (EMBS ’07), pp. 3136–3139, 2007.

[51] I. Maglogiannis, E. Zafiropoulos, and C. Kyranoudis, “Intelligent segmentation and classification of pigmented skin lesions in dermatological images,” in Advances in Artificial Intelligence, G. Antoniou, G. A. Potamias, C. Spyropoulos, and D. Plexousakis, Eds., vol. 3955 of Lecture Notes in Computer Science, pp. 214–223, Springer, Berlin, Germany, 2006.

[52] Mryka Hall-Beyer, “The GLCM Tutorial,” Available online: http://www.fp.ucalgary.ca/mhallbey, Website Referenced on August 15, 2016.

[53] T. Tanaka, S. Torii, I. Kabuta, K. Shimizu, M. Tanaka, and H. Oka, “Pattern classification of nevus with texture analysis,” in Proceedings of the 26th Annual International Conference of the IEEE Engineering in Medicine and Biology Society (EMBC ’04), pp. 1459–1462, 2004.

[54] H. Zhou, M. Chen, and J. M. Rehg, “Dermoscopic interest point detector and descriptor,” in Proceedings of the 6th IEEE International Symposium on Biomedical Imaging: From Nano to Macro (ISBI ’09), pp. 1318–1321, 2009.

[55] C. Lee and D. A. Landgrebe, “Decision boundary feature extraction for neural networks,” IEEE Transactions on Neural Networks,vol. 8, no. 1, pp. 75–83, 1997.

[56] C. Lee and D. A. Landgrebe, “Decision boundary feature extraction for nonparametric classification,” IEEE Transactions on Systems, Man and Cybernetics, vol. 23, no. 2, pp. 433–444, 1993.

[57] C. Lee and D. A. Landgrebe, “Feature extraction based on decision boundaries,” IEEE Transactions on Pattern Analysis and Machine Intelligence, vol. 15, no. 4, pp. 388–400, 1993.

[58] Ammara Masood and Adel Ali Al- Jumaily, “Computer Aided Diagnostic Support System for Skin Cancer: A Review of Techniques and Algorithms,” Int. Journal of Biomedical Imaging, 2013.

[59] V.P. Gladis Pushpa Rathi and S. Palani “A Novel Approach for Feature Extraction and Selection on MRI Images for Brain Tumor Classification,” Conf. on Computer Science, Engineering and Apllications, pp. 225-234, 2012.

[60] Marc Wieland and Massimiliano Pittore “Performance Evaluation of Machine Learning Algorithms for Urban Pattern Recognition from Multi-Spectral Satellite Images,” remote sens. Vol. 6, pp. 2912-2939, 2014.

[61] Jose M. P. Nascimento and Jose M. Bioucas Dias “Vertex Component Analysis: A Fast Algorithm to unmix Hyperspectral Data,” IEEE Transactions on Geoscience and Remote Sensing, Vol. 43, No. 4, pp. 898-910, 2005.

[62] M. Miljkovic, L. Quintero, C.Matthaus, T. Chernenko and M. Diem "A Comparison of Imaging Algorithms for the Analysis of Raman Hyperspectral Datasets from Human Cells," Available online: http://www.censsis.neu.edu/sitevisit2009/posters2009/R2C_p2.pdf, Website Referenced on May 16, 2016.

[63] Xianghua Xie "A Review of Recent Advances in Surface Defect Detection using Texture analysis techniques," ELCVIA, Vol. 3, 2008.

[64] Haralick RM, Shanmugam K, and Dinstein IH "Textural features for image classification," IEEE Transactions on Systems, Man and Cybernetics, pp. 610-621, 1973.

[65] Madison Kretzler "Automated Curved Hair Detection and Removal in Skin Images to support Automated Melanoma Detection," MSc dissertation, 2013.

[66] Michal Kruk, Bartosz Swiderski, Stanislaw Osowski, Jaroslaw Kurek, Monika Slowinska and Irena Walecka "Melanoma recognition using extended set of descriptors and classifiers," EURASIP journal on Image and Video Processing, 2015.

[67] Nikita Singh and Alka Jindal "A Segmentation method and Comparison of Classification Methods for Thyroid Ultrasound Images," Research Gate, 2012.

[68] Fritz Albregtsen "Statistical texture Measures Computed from Gray Level Co-occurrence matrices," 2008.

[69] Mariam A. Sheha, Mai S. Mabrouk and Amr Sharawy "Automatic Detection of Melanoma Skin Cancer using Texture Analysis," Int. Journal of Computer Applications, Vol. 42, No. 20, pp. 22-26, 2012.

[70] Samy Bakheet "An SVM framework for Malignant Melanoma Detection Based on Optimized HOG Features," Vol. 4, 2017.

[71] El- Naqa, Yanq Y, Wernick MN, Galatsanos NP, Nishikawa RM 'A support vector machine approach for detection of microcalcifications," IEEE Trans Med Imaging, pp. 1552-1563, 2002.

[72] Lacarrubba F, D'Amico V, Nasca M R, Dinotta F, Micali G. "Use of dermatoscopy and video dermatoscopy in therapeutic follow-up: a review," Int. journal of dermatology, pp. 866-873, 2010.

[73] Amanda Oakley "Dermatoscopy," Available online: www.dermnetnz.org/cme/dermoscopy-course/introduction-to-dermoscopy/, Website Referenced on February 23, 2017.

[74] K. C. Nischal and Uday Khopkar "Dermoscope," Indian Journal on Dermatol venereol Leprol, vol.71, pp. 300-303, 2005.

[75] S. Sachdeva, "Fitzpatrick skin typing: Applications in dermatology," Indian Journal on Dermatol Venereol Leprol., vol. 75, no. 1, pp. 93–96, 2009.

[76] Teresa Mendonca, pedro M. Ferreira, Jorge S. Marques, Andre R.S. Marcal and Jorge Rozeira "PH^2 – A dermoscopic image database for research and benchmarking," 2011.

[77] M. Partridge and R. Calvo,"A fast dimensionality reduction and simple PCA," Intel. Data Anal, pp. 203-214, 1998.

[78] H. Wang, X.-H. Wang, Y. Zhou, J. Yang, "Color texture segmentation using quaternion-Gabor filters," IEEE International Conference on Image Processing, pp.745–748, 2006.

[79] L. Shi, B. Funt, "Quaternion color texture segmentation," Comput. Vision Image Understanding, vol. 107 (1–2), pp. 88–96, 2007.

[80] Muliye Kibabew "Artifact Detection in Endoscopic Bowel Images Using Image Processing," M.S. Thesis, 2016.

[81] B. Miroslav, H. Robert, "Novel Method for Color Textures Features Extraction Based on GLCM," Radioengineering, Vol. 16, No. 4, December 2007.

[82] Pirnog I., Preda R. O., Oprea C., and Paleologu C. "Automatic lesion segmentation for melanoma diagnostics in macroscopic images," IEEE Trans on Signal Processing Conference, pp. 659-663, 2015.